US Army Corps of Engineers

GEOTECHNICAL LABORATORY

MISCELLANEOUS PAPER S-73-1

STATE-OF-THE-ART FOR ASSESSING EARTHQUAKE HAZARDS IN THE UNITED STATES

Report 27

EVALUATION OF GROUND FAILURE DISPLACEMENT ASSOCIATED WITH SOIL LIQUEFACTION: COMPILATION OF CASE HISTORIES

by

Steven F. Bartlett, T. Leslie Youd

Department of Civil Engineering
Brigham Young University
Provo, Utah 84602

February 1990
Report 27 of a Series

Prepared for DEPARTMENT OF THE ARMY
US Army Corps of Engineers
Washington, DC 20314-1000
Under Contract No. DACW39-87-M-2007
Monitored by Geotechnical Laboratory
US Army Engineer Waterways Experiment Station
3909 Halls Ferry Road, Vicksburg, Mississippi 39180-6199

Unclassified
SECURITY CLASSIFICATION OF THIS PAGE

REPORT DOCUMENTATION PAGE

Form Approved OMB No. 0704-0188

1a. REPORT SECURITY CLASSIFICATION Unclassified	1b. RESTRICTIVE MARKINGS
2a. SECURITY CLASSIFICATION AUTHORITY	3. DISTRIBUTION/AVAILABILITY OF REPORT Approved for public release; distribution unlimited.
2b. DECLASSIFICATION/DOWNGRADING SCHEDULE	
4. PERFORMING ORGANIZATION REPORT NUMBER(S)	5. MONITORING ORGANIZATION REPORT NUMBER(S) Miscellaneous Paper S-73-1
6a. NAME OF PERFORMING ORGANIZATION Department of Civil Engineering Brigham Young University 6b. OFFICE SYMBOL (If applicable)	7a. NAME OF MONITORING ORGANIZATION USAEWES Geotechnical Laboratory
6c. ADDRESS (City, State, and ZIP Code) Provo, UT 84602	7b. ADDRESS (City, State, and ZIP Code) 3909 Halls Ferry Road Vicksburg, MS 39180-6199
8a. NAME OF FUNDING/SPONSORING ORGANIZATION US Army Corps of Engineers 8b. OFFICE SYMBOL (If applicable)	9. PROCUREMENT INSTRUMENT IDENTIFICATION NUMBER Contract No. DACW39-87-M-2007
8c. ADDRESS (City, State, and ZIP Code) Washington, DC 20314-1000	10. SOURCE OF FUNDING NUMBERS PROGRAM ELEMENT NO. / PROJECT NO. / TASK NO. / WORK UNIT ACCESSION NO.

11. TITLE (Include Security Classification) State-of-the-Art for Assessing Earthquake Hazards in the United States; Report 27, Evaluation of Ground Failure Displacement Associated with Soil Liquefaction: Compilation of Case Histories

12. PERSONAL AUTHOR(S)
Bartlett, Steven, F., Youd, T. Leslie

13a. TYPE OF REPORT	13b. TIME COVERED	14. DATE OF REPORT (Year, Month, Day)	15. PAGE COUNT
Report 27 of a Series	FROM _____ TO _____	February 1990	88

16. SUPPLEMENTARY NOTATION
Available from National Technical Information Service, 5285 Port Royal Road, Springfield, VA 22161.

17. COSATI CODES		
FIELD	GROUP	SUB-GROUP

18. SUBJECT TERMS (Continue on reverse if necessary and identify by block number)
Earthquakes
Land spreading
Liquefaction displacement
Soil deformation
Soil liquefaction

19. ABSTRACT (Continue on reverse if necessary and identify by block number)

Liquefaction induced ground failure is responsible for considerable damage to engineering structures during major earthquakes. ~~At~~ present, only a few empirical models exist for predicting the amount of horizontal displacement resulting from liquefaction, and None of the present empirical models has fully addressed both seismic and site factors which influence horizontal displacement. This study compiles

The purpose of this investigation is to compile case histories of liquefaction induced ground failure and tabulate seismic, geological, topographical, and soil properties that may affect permanent horizontal ground displacement to provide a data set for the development of empirical predictive models. Case histories of lateral spreading gleaned from reports on the 1906 San Francisco, 1964 Alaska, 1964 Niigata, 1971 San Fernando, 1979 Imperial Valley, 1983 Nihonkai-Chubu, 1983 Borah Peak, Idaho, and 1987
(Continued)

20. DISTRIBUTION/AVAILABILITY OF ABSTRACT	21. ABSTRACT SECURITY CLASSIFICATION
☒ UNCLASSIFIED/UNLIMITED ☐ SAME AS RPT. ☐ DTIC USERS	Unclassified
22a. NAME OF RESPONSIBLE INDIVIDUAL	22b TELEPHONE (Include Area Code) / 22c. OFFICE SYMBOL

19. ABSTRACT (Continued).

Superstition Hills earthquakes are compiled (appendix to this report, Bartlett and Youd, 1989a). Techniques used to estimate pertinent measures that were not measured or documented in the original studies (e.g. many maximum site accelerations, strong ground motion duration, and thickness of liquefiable sediments) are also presented.

Additionally, preliminary correlation regression analyses are done on the more pertinent measures to discover their value as predictor (i.e. independent) variables. The duration of strong ground motion and the thickness of the liquefied zone divided by the depth to the top of the liquefied zone are significant predictors of horizontal ground displacement at the 95 percent confidence level. Topographical factors and mean grain size also appear to influence horizontal ground displacement.

PREFACE

This report was prepared by Steven F. Bartlett and Prof. T. Lesslie Youd, Brigham Young University (BYU), Provo, Utah, under Contract DACW39-87-M-2007.

Masanori Hamada of Tokai University, Shimizu, Japan, provided the cross sections for liquefaction sites from the 1964 Niigata and 1983 Nihonkai-Chubu earthquakes. Sheryl Bartlett assisted in the preparation of the figures for this report.

This report was prepared under the direct supervision of Dr. E. L. Krinitzsky, Engineering Geology and Rock Mechanics Division (EGRMD), Geotechnical Laboratory (GL), US Army Engineer Waterways Experiment Station (WES), and the general supervision of Dr. A. G. Franklin, Chief, EGRMD, and Dr. W. F. Marcuson III, Chief, GL.

The appendix to this report, Bartlett and Youd, 1989a, BYU Civil Engineering Department Report No. CEG 89-01, which contains the tabulated data for the researched case histories is available upon request.

COL Larry B. Fulton, EN, is the present Commander and Director of WES. Dr. Robert W. Whalin is Technical Director.

TABLE OF CONTENTS

LIST OF FIGURES

LIST OF FIGURES CONTINUED

LIST OF TABLES

CHAPTER 1: INTRODUCTION

Much of the damage to structures during major earthquakes can be attributed to ground failure caused by soil liquefaction. Lateral spreading on gentle slopes of less than five percent is probably the most common and pervasive type of liquefaction induced ground failure. Lateral spreading during the 1964 Alaskan Earthquake caused $50 million damage (1964 value) to 266 bridges of the Trans-Alaskan railroad and highway as well as disrupting buildings, pipelines and other constructed works. Total ground failure displacement damage for the Alaskan earthquake may have reached $300 million (Youd, 1978). Lateral spreading during the 1906 San Francisco earthquake damaged several buildings, roads and bridges. Perhaps more importantly, buried water mains for the downtown area were severed by lateral spreading. The resulting loss of water greatly hampered fire fighting efforts during the ensuing fire.

There are two general questions that must be resolved when attempting to evaluate a site for a possible liquefaction induced ground failure: 1) Are sediments within the soil profile susceptible to liquefaction? 2) Once liquefaction has occurred, how much displacement and damage is possible. Much research has been generated since the 1964 Niigata and 1964 Alaskan earthquakes in attempting to resolve the first question. However, only limited progress has been made in trying to quantify the potential permanent horizontal ground displacement.

The National Research Council, 1985, in outlining new initiatives in liquefaction research states, "There are a number of research needs that have recently emerged as being important [including] . . . 3. Methods of

evaluating the magnitude of permanent soil deformations induced by earthquake shaking, while considered in the past, have emerged as a pressing need to understand the dynamic behavior of structures and soil deposits. Both triggering and dynamic soil strength must be considered in studying the effect of liquefaction or high pore pressure on deformations. Calculations based on realistic constitutive models are needed to help comprehend the development of permanent deformations and progressive failure (p. 217)."

This paper reviews past work regarding liquefaction induced horizontal ground displacement, identifies pertinent seismic, geological and soil factors that influence lateral spreading, compiles case histories of lateral spreading during major earthquakes and evaluates some possible regression models that estimate permanent horizontal ground displacement. Although other types of failures are important (i.e., flow failure, ground oscillations, bearing capacity failure, settlement and buoyant rise of buried structures), this study is limited to researching lateral spreading.

These documented case histories of lateral spreading (appendix to this report, Bartlett and Youd, 1989a, Brigham Young University Civil Engineering Dept. Report No. CEG 89-01) provide: 1) field observations from which factors controlling lateral spreading may be evaluated and 2) a database of documented and estimated values for the development and verification of empirical, analytical and numerical models that predict permanent horizontal ground displacement. Formulation of functional empirical models will allow calculation of potential horizontal ground displacements at specific engineering sites. The estimation of potential displacement is important to designers appraising the risk involved in construction of new facilities or mitigating the threat to existing facilities in earthquake prone regions.

CHAPTER 2: BACKGROUND INFORMATION AND PAST WORK

2.1 Introduction

In this study, liquefaction is defined as a significant loss of soil shear strength due to a transient rise in pore pressures resulting from strong ground shaking. Liquefaction induced ground failure is any displacement, settlement or loss of the soil's bearing capacity resulting from a decline in the soil's effective strength.

The National Research Council, 1985, recognizes two distinct ground deformation behaviors resulting from earthquake induced liquefaction: flow failure and deformation failure. In the following sections, flow failure and deformation failure are defined and contrasted. Mechanisms which might explain how deformation failure occurs are discussed. The morphology of lateral spreading, which is a type of deformation failure, is described. Current empirical models used to estimate horizontal ground displacement resulting from lateral spreading are also reviewed.

2.2 Flow Failure versus Deformation Failure

Permanent ground deformation resulting from **flow failure** is catastrophic and very destructive to constructed works. During flow failure, a liquefied soil is subjected to continuous, very large, shear deformation and flows until arrested by a decrease in ground slope or other impedient to flow. Characteristically, the fluid mass comes to rest as a lobate deposit at the base of a hill or within a topographical depression or stream channel. Flow failures may travel downslope at speeds of tens of miles per hour and cause the soil mass to displace tens to hundreds of feet (Youd, 1978). Generally,

flow failure results when pre-existing static shear stresses are greater than the steady-state (or residual) strength of the soil (NRC, 1985). If the combination of earthquake and static forces can cause the soil to fail, then the residual strength of the soil is insufficient to arrest further deformation and the soil will flow. Flow failure used in this context most nearly matches some of the original definitions of liquefaction. Casagrande, 1936, 1938, considered liquefaction as the collapse and flow of an unstable soil under static stresses. Terzaghi and Peck, 1948, defined liquefaction as the "sudden decrease of shearing resistance of a quick sand from its normal value to almost zero without the aid of seepage pressures."

Deformation failure is characterized by smaller, more limited deformation where the soil mass remains mostly intact during and after strong ground shaking. However, deformation failure may also involve permanent ground deformation that is large enough to be deleterious to many constructed works. Castro, 1969, Castro and Poulos, 1977, NRC, 1985 used the term "cyclic mobility" to describe a process through which dynamic pore pressure generation could reduce the effective strength of a cohesionless soil sufficiently enough to achieve limited deformation under transient dynamic and sustained static loading without producing fluid flow. Three processes have been proposed to explain how deformation failure may be achieved (NRC, 1985).

1) An attempt is made to apply a cyclic stress that, together with the sustained static stress, is greater than the maximum shear resistance of the soil. When the combined stress reaches the maximum resistance plastic flow begins to occur. If the soil is transmitting stress to a mass that can move together, as soil within an infinite slope, the amount of plastic deformation will be determined by the interval of time over which the excessive stress acts.

2) The combined static plus cyclic stress remains less than the maximum resistance of the soil. Permanent deformation accumulates gradually as a result of the rearrangement of soil particles.

3) The sustained static stress acting upon the element increases as a result of the cyclic loading because additional stress has been transferred to the element from other portions of the soil mass that have decreased in stiffness.

In general, deformation failure appears to result when a soil mass loses some of its shear strength due to a transient rise in pore pressures during cyclic loading. Once strong ground motion has ceased, or shortly thereafter, the residual strength of the soil appears to be sufficient to arrest further deformation by the sustained static loads and flow failure does not ensue.

However, the nature, degree and distribution of shear strength loss within the soil profile that occurs during deformation failure is not well understood. Additionally, the effects of both earthquake and static forces acting upon a composite system of liquefied and non-liquefied soil is difficult to analyze. It is possible that shear strength loss during deformation failure may be similar to the shear strength loss during flow failure (i.e., the effective overburden pressure somewhere in the soil profile may approach zero in both cases). Holzer et al., 1989, have reported a case of deformation failure where instrumented pore pressure approached the total overburden pressure. Thus, the degree of shear strength loss may not ultimately determine if a mobilized soil mass undergoes flow or deformation failure.

Whether the soil mass flows or undergoes deformation failure may ultimately be a result of differences in the magnitude and duration of the dynamic and static mobilizing forces as well as the extent, continuity and boundary conditions surrounding the liquefied zone. The magnitude of the mobilizing forces is controlled by the ground slope, the intensity of ground motion and the weight of the overlying soil and any structures placed on the

soil. Deformation failures are likely to occur on gentle slopes where static shear stresses are smaller than the viscous strength of the liquefied soil. Additionally, disrupted layers, lenses, and other heterogeneities and discontinuities affect the areal and cross-sectional extent of the liquefied zone and increase or decrease the forces resisting mobilization. Furthermore, the depth and thickness of the liquefied layer within the soil profile may influence whether or not the mobilized mass flows or moves as a deformation failure. For example, if the liquefied layer is thick relative to the overlying unliquified surface layer, the thin crust of the unliquefied surface layer may offer little resistance to mobilization and be engulfed in the flow as the failure moves downslope. However, if liquefied layer is thinner and deeper, the overlying unliquefied surface layer may offer more resistance to mobilization and the soil column might remain mostly intact as the soil mass migrates downslope. Thus, liquefaction occurring at a greater depth may produce features commonly attributed to deformation failure.

2.3 Liquefaction Induced Lateral Spreading

Lateral spreading is a type of deformation failure resulting from liquefaction. During lateral spreading, surficial soil layers displace down gentle slopes along some shearing zone where the soil strength has been sufficiently reduced by a transient rise in pore water pressure to permit movement (Figure 1). The lateral displacement may be caused by gravitational or seismic forces or a combination of both. The soil layers above the liquefied zone generally retain their strength and ride passively on underlying weakened soil. Typically, lateral spreading occurs on gentle slopes ranging from 0.5 to 5 percent (Youd, 1978). Morphologically, such a

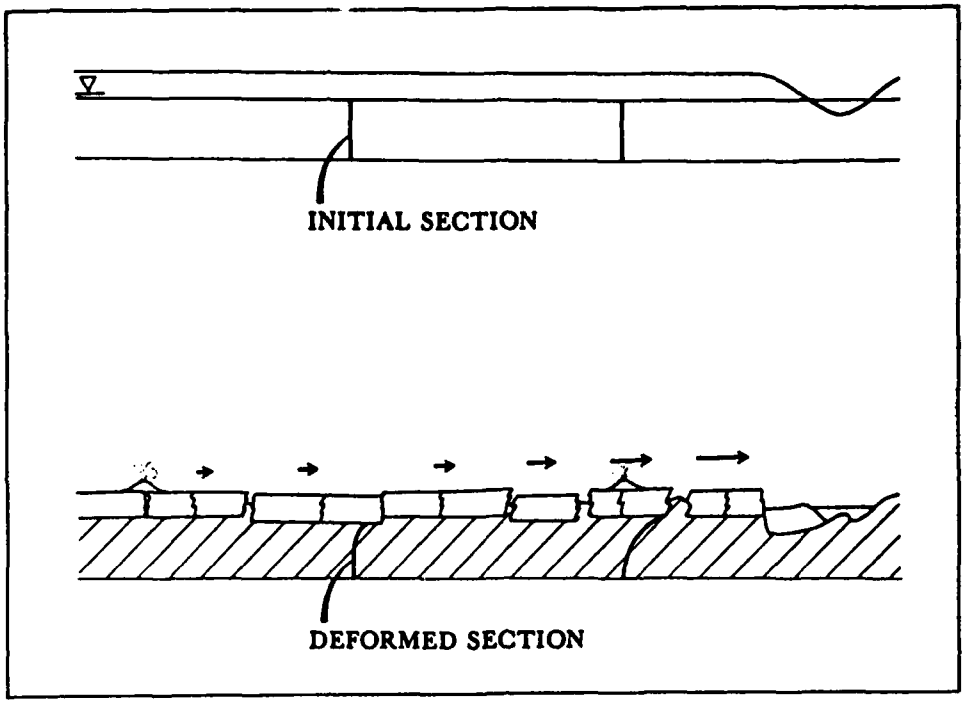

Figure 1 Block Diagram of Lateral Spreading

failure, termed a "lateral spread", typically consists of a zone of displaced soil with extensional fissures at the head, shear deformations at the side margins, and compression or buckling of the soil near the toe. Buried objects such as pipelines, piles, etc. are often sheared by differential movement within the lateral spread. Structures at the head are commonly pulled apart and those at the toe are compressed or buckled.

2.4 Other Types of Liquefaction Induced Ground Failure

Although not addressed by this study, other types of liquefaction induced ground failure are recognized and are described for classification purposes. When no slope is present, the liquefied soil may oscillate back and forth in response to earthquake wave motion, but no net horizontal movement is achieved. Such ground oscillations, though transitory, may be

damaging to pipelines and other rigid structures that lie on or within the oscillating zone. **Ground settlement** may also occur as the soil compacts when it reconsolidates. Such action produces settlement of the ground surface often accompanied by fissures and sand boils. Liquefied sands can reduce the bearing capacity of the soil. **Bearing capacity failure** may result causing structures to settle, tip and even overturn. Conversely, objects lighter than the liquefied soils may buoyantly rise.

2.5 Past and Current Work on Prediction of Liquefaction Induced Horizontal Ground Displacement

This section reviews some of the past work on estimation of permanent horizontal ground displacement resulting from lateral spreading. A review of past work provides: 1) insight into which seismic and site factors may be influencing horizontal ground displacement, and 2) ideas on how these factors may be expressed in empirical models.

Several authors have introduced predictive models based on empirical, analytical and numerical techniques. Newmark, 1965, and later expanded by Goodman and Seed, 1966, and Makdisi and Seed, 1978, outlined various procedures to estimate permanent ground displacement using sliding block analysis. Youd and Perkins, 1987, developed an empirical equation to predict maximum horizontal ground displacement based on earthquake magnitude and distance to the zone of seismic energy release. Ishihara, 1985, presented a set of curves which predict the potential for liquefaction induced ground damage based on the thickness of the liquefiable layer compared to the thickness of the overlying unliquefied layer. Finally, Hamada, et al., 1986, presented a regression formula to predict horizontal ground displacement based

on slope and estimates of the thickness of the liquefied layer from measurements taken from liquefaction sites during two Japanese earthquakes.

2.5.1 Newmark Sliding Block Analysis, 1965

Newmark, 1965, Goodman and Seed, 1966 and Makdisi and Seed, 1978, explained how sliding block analysis can be used to estimate permanent ground displacement if the soil's shear strength loss during strong ground motion is not too great (i.e., flow failure does not occur). A potential failure surface within the slope is first analyzed statically to determine what earthquake acceleration is needed to produce equilibrium and to initiate failure. If at some time during the earthquake, the horizontal acceleration exceeds the undrained shear strength of the soil, the soil block will translate downslope along the failure surface. (Upslope translation of the block during stress reversals is not likely because downslope forces are generally too great to allow upslope movement). The net movement downslope is governed by the shear strength of the soil along the failure surface during cyclic loading and the intensity and time interval during which inertial driving forces act. The undrained shear strength of the soil during cyclic loading is a function of the pore pressure build up and the amount of strain experienced by the soil. Newmark, 1965, suggests the use of an average undrained shear strength along the failure surface for estimating displacement. For worst case conditions, the residual strength may be used for the average undrained shear strength.

2.5.2 Youd - Perkins Liquefaction Severity Index, 1987

Youd and Perkins, 1978, 1987, Youd 1989, noted that the severity of

damage from liquefaction is a function of the type of failure (e.g. flow failure, lateral spreading, ground oscillation, etc.) and the amount of permanent horizontal ground displacement. Buildings and other structures subjected to 2 to 4 inches of permanent horizontal ground displacement usually incurred little or reparable damage; structures subjected to 5 to 24 inches of displacement generally incurred minor to major damage and structures subject to greater than 30 inches of displacement incurred major damage.

Youd and Perkins also identified several seismological, sedimentological, topographical, hydrological and engineering factors which they feel influence liquefaction and ground failure. The seismological factors listed are: 1) the **intensity of ground motion** and 2) the **duration of the ground motion**. The sedimentological factors identified are: 1) the **thickness of the liquefied layer**, 2) the **areal extent** of the liquefied layer, 3) the **confinement** of the layer **by impermeable sediments**, 4) the **age** of the sediments, 5) the **degree of lithification or cementation** and 6) the **mode of deposition**. The topographical factors listed are: 1) the **ground slope** and 2) the **nearness of the failure to a free face** (e.g. stream channel or other abrupt topographical depression). The hydrological factors mentioned are: 1) the **depth to ground water** and 2) the presence of **artesian pressure**. The engineering factors they considered important are: 1) the soil's **grain size**, 2) the soil's **relative density** (as measured by some subsurface testing such as the standard penetration test or cone penetration test) and 3) the **fabric or packing** of the soil.

Youd and Perkins evaluated the liquefaction severity for cases of liquefaction induced ground failure that occurred in a particular type setting. They limited their evaluation to lateral spreading of saturated

cohesionless gently sloping holocene fluvial or deltaic deposits in rivers with channels widths greater than 10 meters and with soil densities that range from 2 to 10 standard penetration blow counts per foot. By applying these restrictions to the case histories considered, the site factors that influence ground displacement (i.e. sedimentological, topographical, hydrological and engineering conditions) are thought to be similar enough so as to control their influence and minimize their significance as predictor variables in a regression analysis.

Youd and Perkins, 1987, named the amount of permanent horizontal ground failure displacement (in inches) the "**liquefaction severity** or **S.**" By selecting a particular geological type setting for their evaluation, the liquefaction severity, S, is essentially a function of the severity of strong ground motion. Seismic factors such as the amplitude of strong ground motion, A, and its duration, D, in seconds are commonly used to characterize the severity of earthquake shaking:

$$S = f(A, D). \qquad (2\text{-}1)$$

The amplitude of strong ground motion, attenuates logarithmically with distance from the seismic energy source (Joyner and Boore, 1981). The duration of strong ground motion, in contrast, shows a slight increase with increasing distance from the source. However, both amplitude and duration of strong ground motion are strongly proportional to the magnitude of the earthquake. Therefore, Youd and Perkins selected to express S in terms of a earthquake magnitude and distance from the energy source:

$$S = f(M_w \ \log R) \qquad (2\text{-}2)$$

where M_w is the moment magnitude and R is the distance from the seismic source in kilometers. The moment magnitude was chosen as the seismic measure because

it better correlates with the total energy released during an earthquake than other measure of magnitude (Kanamori, 1978).

Youd and Perkins introduced the liquefaction severity index, LSI, as a convenient scale to estimate the **maximum** amount of permanent ground displacement occurring within the defined type section for a given seismic event. The liquefaction severity index was chosen to range between 0 inches to a limiting maximum of 100 inches. Past displacements greater than 100 inches were considered to be so damaging and erratic in nature that extending the LSI beyond 100 inches is not necessary. Youd and Perkins selected a best estimate of the **maximum** permanent horizontal ground displacement reported for a particular case history as an measure of the potential ground failure hazard for that locality. The localities where the reported horizontal ground displacement obviously exceeded 100 inches were assigned a limiting LSI of 100 and were excluded from their regression analysis.

In developing a predictive equation for the LSI, Youd and Perkins expressed the seismic factors in terms of a magnitude-distance non-linear model. Least squares regression was used to determine an empirical equation from the data presented in Table 1.

These data fitted the following equation:

$$\log LSI = -3.49 - 1.86 \log R + 0.98 M_w \qquad (2\text{-}3)$$

where LSI equals the maximum permanent horizontal displacement in inches, R equals the horizontal distance from the energy source in kilometers and M_w is the moment magnitude.

Youd and Perkins used this function in conjunction with a seismic zone model to compile a liquefaction severity index map for southern California.

TABLE 1

Magnitude, Distance and LSI for Various Liquefied Sites
(data from Youd, Perkins 1987)

Locality	Mw	Dist. (km)	LSI (in)
San Ardo	8.1	95	5
Gonzales Bridge	8.1	44	20
Salinas Bridge	8.1	27	70
Neponsat Bridge	8.1	24	100
Moss Landing	8.1	18	100
McGowan Ranch	8.1	15	100
Witcomb Ranch	8.1	27	70
Duncan's Mill	8.1	10	100
Healdsbrug	8.1	33	25
Alexander Valley	8.1	41	15
Eel River Delta	8.1	40	30
Valdez	9.2	0	100
Yakataga	9.2	5	100
Seward	9.2	18	100
Snow River	9.2	48	100
Hunter Flats	9.2	50	60
Portage	9.2	50	100
Elkutna River	9.2	110	60
Matanuska River	9.2	110	50
Beluga Lake	9.2	210	15
Fairbanks	9.2	420	2
Ranch	6.9	10	30
Leslie	6.9	38	2
Wiest Lake	6.5	12	7
Hwy 2, Mexico	6.5	16	5
San Felepe Creek	6.5	34	1
Callegua Creek	5.75	5	5
Magu Lagoon	5.75	7	2
Highway 111	5.6	5	2
Radio Tower	5.6	11	1
Goleta Point	5.2	8	2

2.5.3 Ishihara, Boundary Curves for Identification of Liquefaction Induced Damage, 1985

Ishihara, 1985, and Goa, 1983, identified areas that had suffered ground failure damage during the 1976 Tangshan and 1983 Nihonkai-Chubu earthquakes from aerial photographs. Ishihara, 1985, proposed that the occurrence of damage from liquefaction induced ground failure is dependent on the thickness of overlying unliquefiable surface layer and the thickness of the liquefiable sand layer. From his study, he defined the thickness of the liquefiable sand layer as the thickness of the sand layer or layers found below the water table with a standard penetration blow count of ten or less (N <= 10, Figure 2). Ishihara plotted the thickness of the overlying unliquefiable surface layer versus the thickness of the liquefiable sand layer for sites of occurrence and non-occurrence of liquefaction induced damage. Boundary lines were drawn for the two earthquakes which divided sites that suffered liquefaction induced damage from sites that showed no evidence of damage (Figure 3). Data points that fall on the left hand side of these curves indicate

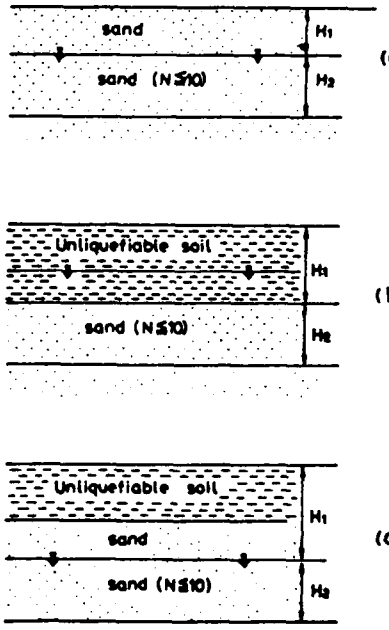

Definitions of the surface unliquefiable layer and the underlying liquefiable sand layer

Figure 2 Definitions of Surface Unliquefiable Layer and the Underlying Liquefiable Sand Layer (Ishihara, 1985).

sites that suffered liquefaction induced damage. The boundary line drawn for the Tangshan earthquake does not intersect the origin of the plot, but swings upward as the thickness of the surface layer decreases. It is not clear why Figure 3 indicates this relationship, but it probably reflects a lack of well defined data for this region of the plot and does not represent actual behavior.

From the data presented in Figure 3, Ishihara, 1985, proposed that the shape of the boundary curves should resemble those shown in Figure 4. Because of the large difference in site accelerations for the two case studies (200 gals for the Nihonkai-Chubu and 400 to 500 gals Tangshan earthquakes), Ishihara included a intermediate boundary line which represents the proposed relationship for site accelerations of 300 gals (Figure 4). Figure 4, therefore provides a method for assessing if liquefaction induced

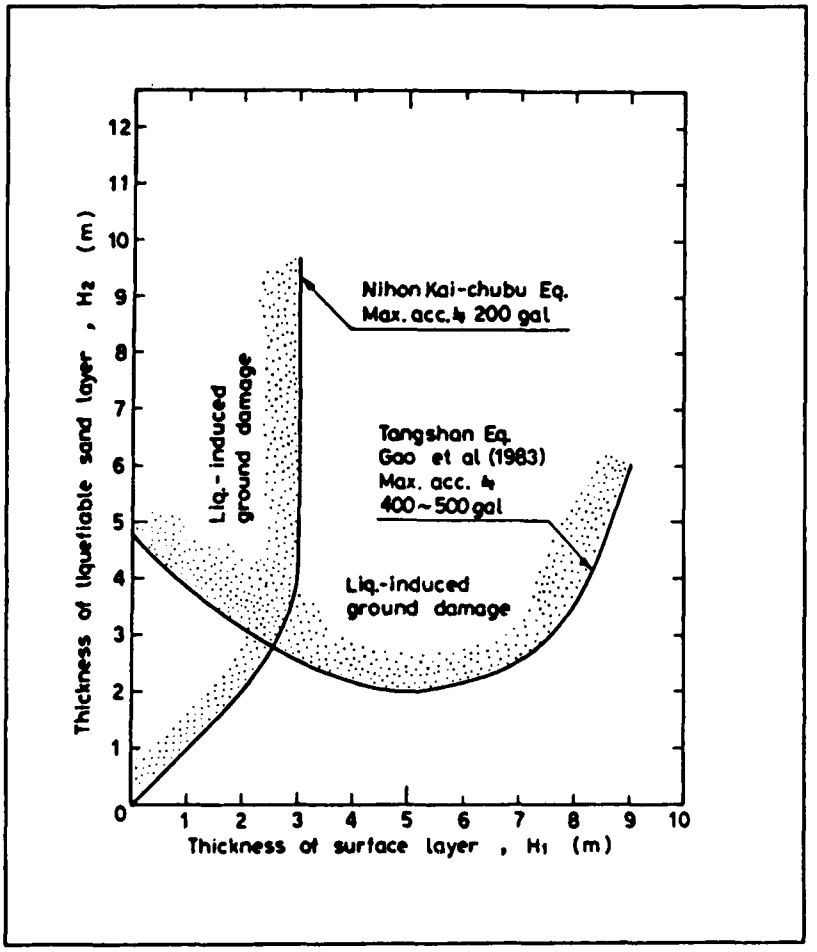

Figure 3 Comparison of Two Boundary Curves Differentiating Conditions of Damage and No Damage Due to Liquefaction (Ishihara, 1985).

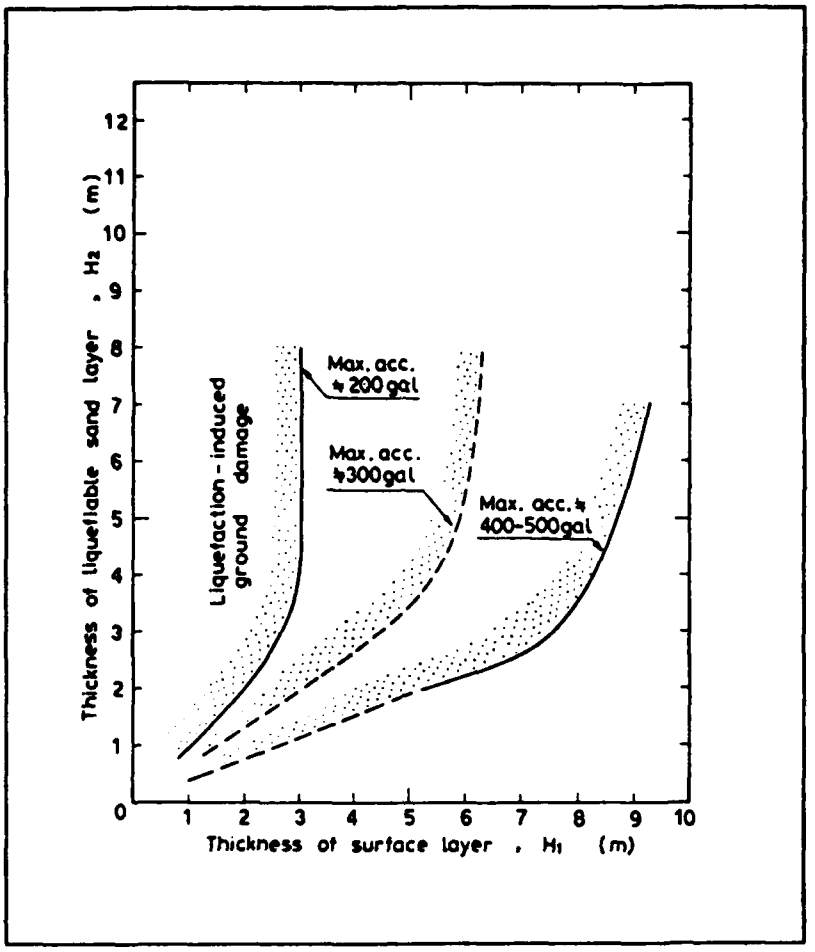

Figure 4 Proposed Boundary Curves for Site Identification of Liquefaction Induced Damage (Ishihara, 1985).

surface damage will occur based on the thickness of the overlying unliquefiable surface layer and the thickness of the underlying liquefiable sand layer. Ishihara's study gave no means of actually estimating the amount of horizontal ground displacement. However, it is important because it suggests that the depth to the liquefiable layer influences displacement and damage.

2.5.4 Hamada et al., 1986, Study on Liquefaction Induced Permanent Ground Displacement

Hamada et al., 1986, used displacement, slope and subsurface data from investigations of the 1964 Niigata, the 1983 Nihonkai-Chubu and the 1971 San Fernando earthquakes to develop a regression model for estimating liquefaction induced permanent horizontal ground displacement. In developing their model, Hamada, et al., considered the following geological and topographical features: 1) the **thickness of the liquefied zone** , 2) the **gradient of the ground slope**, 3) the **gradient of the liquefied zone** (gradients of upper and lower boundaries of the liquefied zone), 4) the **depth of the liquefied soil zone** (depth to upper and lower boundary of liquefied zone), 5) the **minimum value of factor of liquefaction resistance, F_L** and 6) the **index of liquefaction potential, P_L**.

As defined by Hamada, et al., 1986, the factor of liquefaction resistance F_L is a factor of safety which compares the liquefaction resistance of the soil to the dynamic shear stresses generated by the earthquake:

$$F_L = R/L \qquad (2\text{-}4)$$

where R is the in-situ resistance of the soil given by curves from the Japanese Code of Bridge Design (see Figure 5) and L is the dynamic shear stresses (Hamada et al., 1986, Appendix III or Iwasaki et al., 1978). The in-situ resistance of the soil R is determined from the standard penetration blow count N, the effective overburden stress rv' and the mean grain size D_{50}

$$R = 0.0882(N/rv'+0.7)^{1/2} + 0.19 \qquad (2\text{-}5)$$

where N is in blows per foot and rv' is in kg/cm^2. This equation is valid for $0.02 \text{ mm} \leq D_{50} \leq 0.05 \text{ mm}$ and

$$R = 0.0882(N/rv'+0.7)^{1/2} + 0.225 \log_{10} 0.35/D_{50} \qquad (2\text{-}6)$$

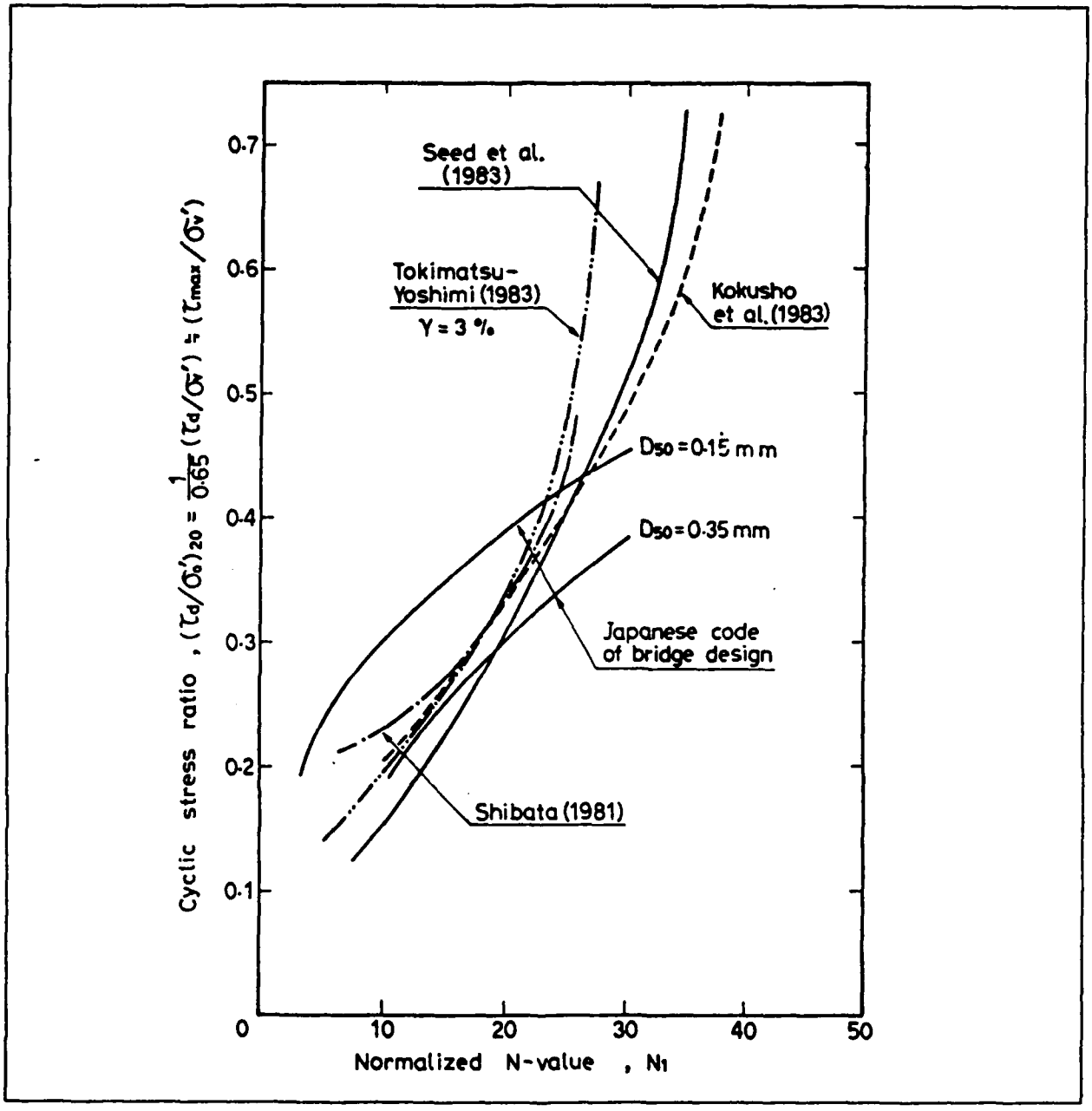

Figure 5 Summary Chart for Evaluating Cyclic Strength Based on the Normalized SPT N-Value (NRC, 1985).

for 0.05 mm \ D_{50} \ 0.6 mm and

$$R = 0.0882(N/rv'+0.7)^{1/2} - 0.05 \qquad (2\text{-}7)$$

for 0.6 mm \ D_{50} \ 1.5 mm. The dynamic earthquake stress is given by:

$$L = ks(rv/rv')r_d \qquad (2\text{-}8)$$

where ks is the seismic coefficient and r_d is a reduction factor for the dynamic shear stress (Hamada, et al., 1986).

The index of liquefaction potential, P_L is defined as:

$$P_L = \text{SUMMATION } (1-F_l)W(z)dz \qquad (2\text{-}9)$$

where $1-F_L$ cannot be less than zero and W(z) = 10 - 0.5z and z is depth (z is restricted to a depth of 20 meters or less for this equation, Hamada et al., 1986). The P_L is influenced by the density of the potentially liquefiable sand and its thickness. The P_L will have a minimum value of 0 if no liquefiable sediments are present in the profile and will have a maximum value of 100 if F_L is 0 for the 20 meters of depth evaluated. The P_L will have high values for thick liquefiable zones with low densities (low SPT N-values) and low values for thin liquefiable zones with high densities (high SPT N-values).

Hamada et al., defined the upper and lower boundary of the liquefied zone throughout the cross section by the factor of resistance, F_L. The zones with a F_L less than one were considered to have liquefied. They interpreted liquefied zone boundaries between the borings so that a continuous cross section could be constructed. If two or more zones liquefied, the total thickness of the liquefied zone was taken to be the sum of the thickness of the individual liquefied zones (Figure 6).

To determine a representative displacement for the cross-section, Hamada et al. divided the cross section into segments which appeared to displace as a unit or block. They averaged the thickness of the liquefied zone(s) in the

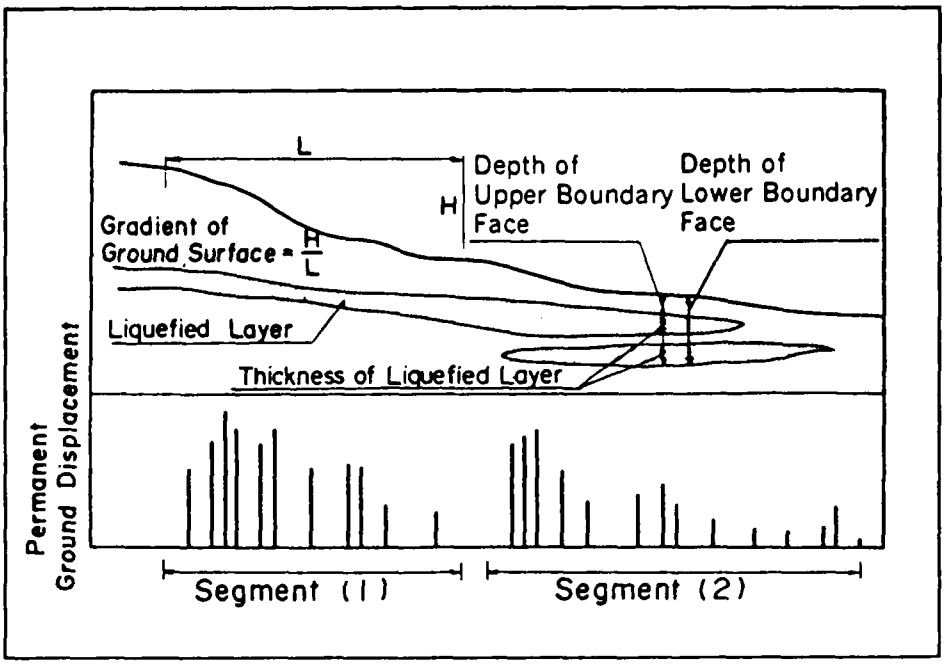

Figure 6 Factors of Liquefied Soil Zone and Topography (Hamada et al., 1986)

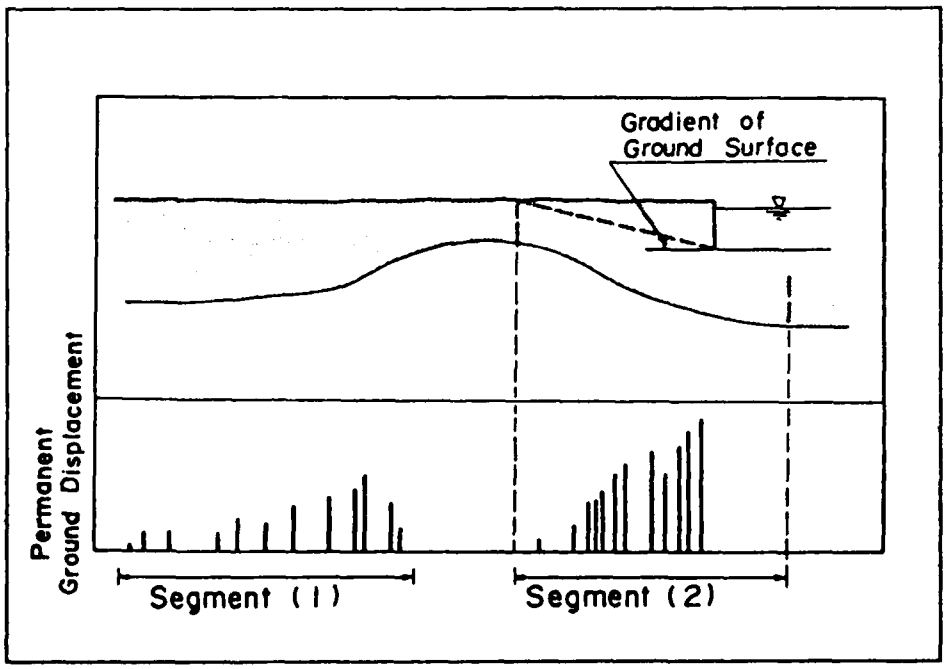

Figure 7 Gradient of Ground Slope Along the Shinano River (Hamada et al., 1986)

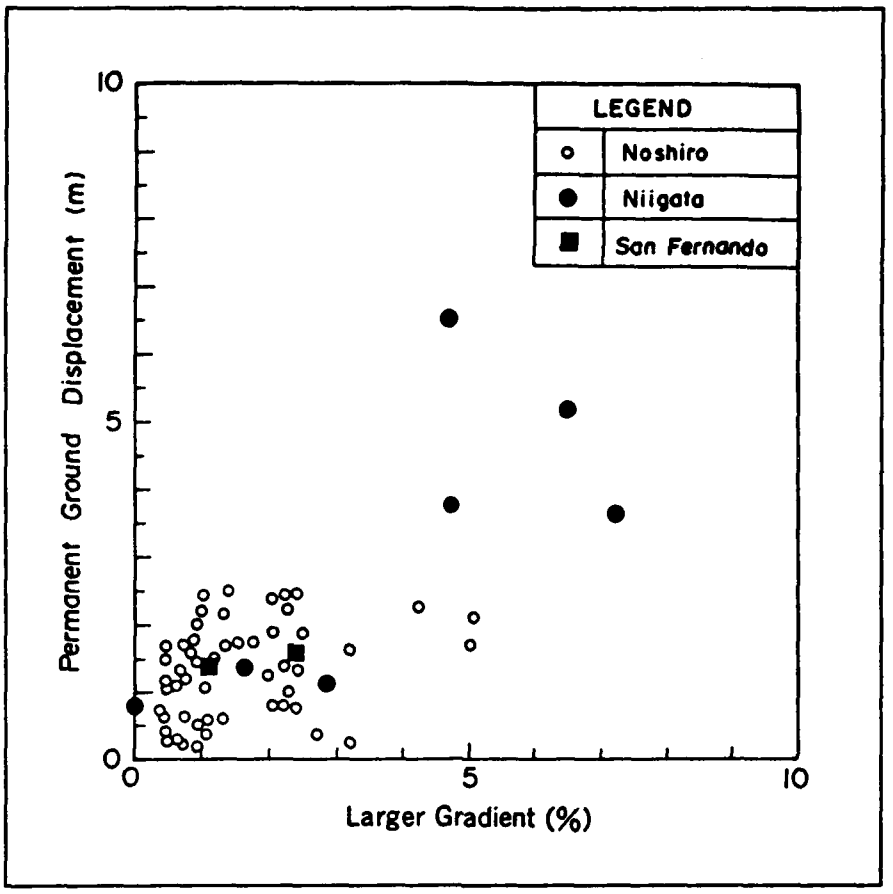

Figure 8 Relationship Between the Largest Value of the Ground Surface Slope and/or the Lower Boundary of the Liquefied Zone and the Measured Permanent Ground Displacement (Hamada et al. 1986)

selected block and the individual vector displacements occurring at the surface of the block and used these averages in their regression analyses. They also averaged the gradient of the ground surface or the gradient of the lower liquefied boundary face (whichever was larger) for each block and used these averages as their slope measurements in the regression analyses. Where a revetment paralleled the river, they considered the slope of the ground surface to be the depth to the bottom of the river channel divided by the horizontal length of the block (Figure 7).

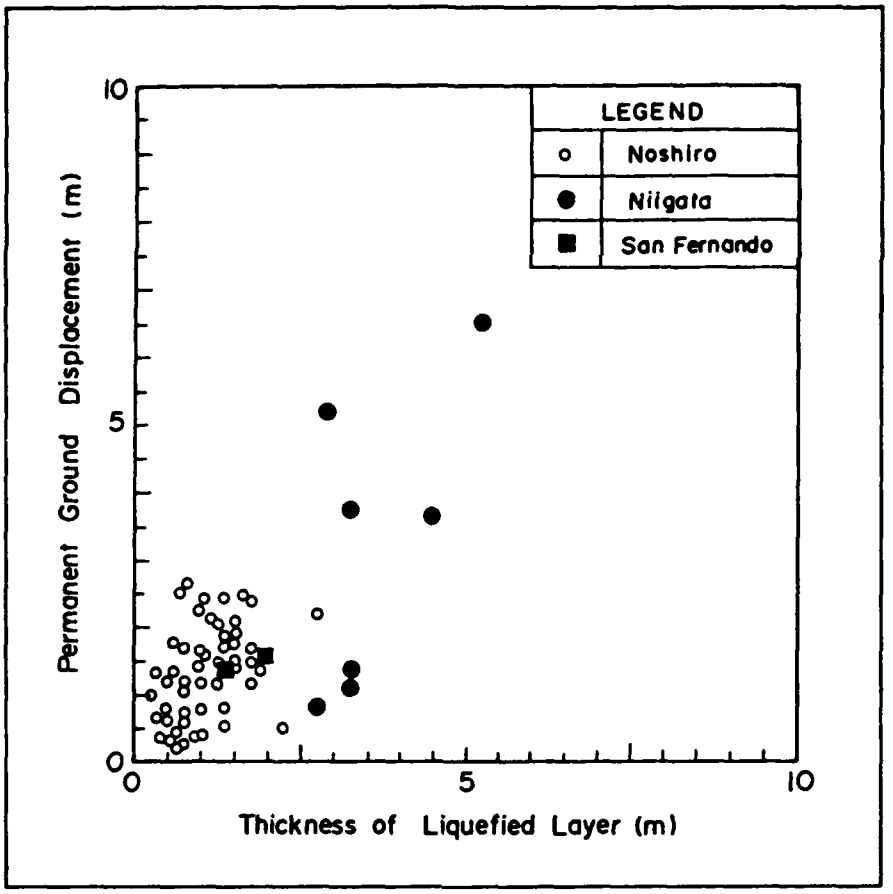

Figure 9 Relationship Between the Measured Permanent Ground Displacement and the Thickness of the Liquefied Zone (Hamada, et al., 1986).

Hamada, et al. found that the larger value of either the slope of the ground surface or the gradient of the lower boundary of the liquefied zone correlated best with displacement (Figure 8). Displacement also correlated reasonably well with the thickness of the liquefied zone (Figure 9). Poorer correlations of F_L and P_L with horizontal displacement were noted.

From these observations, Hamada et al., 1986, developed the following regression equation:

$$D = 0.75\ H^{0.48} S^{0.33} \qquad (2\text{-}10)$$

where D is the horizontal displacement in meters, H is the thickness of the

liquefied zone in meters, and S is the larger of the gradient of the ground surface or the lower boundary face of the liquefied zone in percent.

2.6 Other Analytical and Numerical Approximations for Estimating Permanent Ground Displacements

Elastic and non-linear dynamic analyses have been used by several researches to estimate the amount of residual strain in a soil mass and to use the accumulated residual strain to estimate the amount of permanent horizontal ground displacement. The use of analytical models to predict liquefaction induced ground displacements is in its infancy and much more research and verification is required to before widely accepted techniques are available to the practicing engineer. A brief summary of the general principles used in dynamic analysis is presented, however, the reader is referred to NRC, 1985 and Finn, 1988 for more detailed summaries.

2.6.1. Approximations from Elastic Theory

If the soil does not undergo significant strength loss, then estimation of the deformation from Newmark sliding block analysis is proper. However, if significant strength loss occurs, the nonlinear hysteretic response of a soil to earthquake motion may be estimated from an equivalent linear damped elastic model if the properties of the model are correctly chosen (Idriss and Seed, 1986b, NRC, 1985, Finn, 1988). Typically, the dependence of the modulus and damping on the strain level is reconciled by iteration until strains calculated from assumed properties match empirically determined stress-strain curves for the particular soil type (Seed and Idriss, 1970, Seed et al., 1986b).

The deformation to the soil mass may be approximated by: 1) calculating the dynamic shear stresses induced by the earthquake (obtained from a equivalent linear damped model) 2) converting the dynamic shear stresses to an equivalent set of uniform cycles, 3) estimating the strain potential of a finite element per cycle from laboratory tests and 4) approximating the amount of permanent deformation from the elemental strains. (Finn, 1988, Seed et al., 1973, Seed et al., 1975, Marr and Christian, 1981, Anderson, 1983, Taniguchi et al., 1983, NRC 1985).

2.6.2 Approximations from Nonlinear Dynamic Analysis

Many procedures and computer programs have been introduce which attempt to directly model the nonlinear hysteretic stress-strain response of soils (Finn, 1980, 1982, 1984, 1985a, 1985b, 1988, Marr et al, 1982, Bouckovalas et al, 1984, NRC 1985). The direct nonlinear method uses low strain moduli and shear strengths obtained from in-situ testing or empirical correlations as input. The direct nonlinear method attempts to follow analytically determined hysteretic stress-strain paths during the cyclic loading-unloading and use the tangent moduli of the paths to estimate the residual strains (Finn, 1988).

Martin et al., 1975, introduced a porewater pressure generation model which made it possible to calculate the porewater pressure increase from the cyclic strain history. This enabled nonlinear models to couple porewater pressure generation with the soil's shear strength degradation and more closely approximate permanent deformation.

2.7 Summary of Current Horizontal Ground Failure Displacement Models

Prediction of liquefaction induced ground displacement is still in its

infancy and is a complex, non-linear problem involving many seismic, geological and soil factors which are difficult to define, quantify and model.

Sliding block analyses have frequently been used in analyzing the stability of earth dams and fills for cases where the soil does not undergo a significant strength loss (i.e., flow failure does not occur). It is possible that sliding block analyses may be able to predict horizontal displacements resulting from lateral spreading if the correct average dynamic shear strength for the liquefied soil is chosen. However, it remains uncertain whether or not present correlations for residual strength are good estimators of a liquefied soil's average dynamic shear strength during mobilization. Displacements calculated from sliding block analyses using residual strength need to be compared with measured displacements from case histories.

The Youd and Perkins liquefaction severity index, 1987, includes seismic factors (magnitude and distance to the source) as predictors of horizontal displacement. However, for the particular type section defined and analyzed, they considered the site factors (topography, layer and soil characteristics) to be relatively uniform so that the influence of site factors on displacement is controlled. Therefore, they do not incorporate site topography, layer and soil factors in their LSI model.

Our initial review of displacements and cross sections from liquefied sites during the 1964 Niigata and 1983 Nihonkai-Chubu earthquakes indicate that horizontal displacements appear to be influenced by ground slope and the thickness of the liquefied zone and these site factors appear to have potential as predictors in a regression model.

The LSI may tend to overpredict some displacements for some case histories for two reasons. First, the displacement measurements used to

formulate the LSI were maximum displacements reported for a liquefaction event occurring at a particular distance from the seismic source. Obviously, there were other less severe displacements that occurred a particular location which were not used by Youd and Perkins to define and formulate the LSI. Second, the type setting defined by Youd and Perkins represents high to moderate range of site conditions favoring liquefaction and large displacement (i.e., saturated geologically recent sands with low blow counts ($N < 10$), located near wide active river channels or flood plains). Liquefaction and displacement has occurred at locations where the site soil conditions are less favorable than defined by the LSI type setting (e.g. liquefaction and displacement of gravelly, alluvial fan sediments during the 1983 Borah Peak Idaho earthquake, Andrus and Youd, 1987, Andrus, 1988 and liquefaction and displacement of gravelly fluvial sediments with high blow counts ($N > 10$) at some sites during the 1964 Alaska Earthquake, McCulloch and Bonilla, 1970). Therefore, displacements estimated from the LSI probably represent an upper bound for likely displacements occurring at a particular location.

In contrast to the LSI, the empirical model proposed by Hamada et al. emphasizes site factors such as slope and thickness of the liquefiable zone, but does not directly evaluate the influence of seismic factors. Youd and Perkins, 1987, have proposed that ground displacements are influenced by maximum acceleration and duration of the strong ground motion. The extrapolation of the Hamada et al., 1986, regression equation to predict displacements for large or small earthquake events or sites that contain silty or gravelly soils may not be prudent. Both the Niigata and Nihonkai-Chubu earthquakes were fairly similar in magnitude (7.5 and 7.7 respectively) and both had similar site characteristics (wide spread fairly uniform medium sized

clean sands). Additionally, Hamada et al., 1986, use the thickness of the liquefied zone as one of the predictor variables in their regression model. Because of the wide acceptance and use of the simplified procedure in the United States, it is more convenient to use it to define the liquefied zone. We will use the simplified procedure to determine thickness of the liquefied zone and verify its significance as a predictor of horizontal ground displacement.

A more comprehensive empirical model for predicting horizontal liquefaction induced ground failure displacement is needed. This model should include seismic factors as well as site specific factors (e.g. geological, topographical, layer and soil properties).

CHAPTER 3: IMPORTANT PROPERTIES AND MEASURES

3. 1 Introduction

This section defines the seismic, geological, stratigraphic and soil factors that have been tabulated for each case study. Because of the size of these data, they have not been published in this report but are available upon request in the appendix (BYU Civil Engineering Dept. Report No. CEG 89-01, Bartlett and Youd, 1989a). Some preliminary analyses are summarized in Chapter 5 using these factors as predictor variables in regression models.

Unfortunately, most of the case histories were not instrumented sites and some data had to be estimated by correlations and other techniques (e.g. maximum site acceleration, strong ground motion duration and thickness of the liquefied zone). Additionally, ground slopes and grain size analyses were not reported for some of the case studies. The techniques used to estimate missing data are discussed in this chapter.

3.2 Seismic, Geological, Stratigraphic and Soil Factors

Many of the factors that are tabulated in BYU CE Dept. Report No. CEG 89-01 were identified by Youd and Perkins, 1987, as being significant factors affecting ground failure displacement. Table 2 lists the factors that have been researched. Because many of the measurements documented by the various authors were mostly reported in English units, we chose to record the reported values in our tabulation in English units as well.

TABLE 2

Important Site Information and Measurements
Recorded in BYU CE Dept. Report No. CEG 89-01

Site Information

- references to sources of information
- site name
- location
- earthquake
- type of failure and extent of damage
- geological setting

Seismic Factors

- earthquake name and date
- magnitude (M_w M_s or M_l)
- distance to nearest seismic source or fault rupture (miles)
- maximum acceleration at site (acceleration of gravity, g)
- duration of strong ground motion (seconds)

Geologic and Stratigraphic Factors

- age of sediment (years before present)
- mode of deposition
- total thickness of unconsolidated sediments (feet)
- horizontal variation of soil in section
- depth to groundwater (feet)
- ground slope (percent)
- proximity to free face (feet)
- thickness of the layers (feet)
- thickness of liquefied zone (feet)
- Low and average blow counts for liquefied zone (N and $(N_1)_{60}$)
- CPT data (tip resistances in kg/cm^2)
- depth to top of liquefied zone (feet)
- depth to low $(N_1)_{60}$ (feet)
- confinement of the liquefied layer by less permeable layers
- areal extent of failure (square feet)
- horizontal displacement (inches)

TABLE 2 CONTINUED

Important Site Information and Measurements

Soil Factors

- soil description (unified classification system when used)
- liquid limit, plastic limit and plastic index
- percentage of fines and clay
- mean grain size (millimeters)

3.2.1 Seismic Factors

3.2.1.1 Earthquake Magnitude - Kanamori, 1978 gives a good review of some the current measures of earthquake magnitude. We report the moment magnitude, M_w when given, as the best estimate of earthquake size. Because the moment magnitude is defined in terms of energy, it is a better representation of earthquake size for many engineering applications than other types of magnitude measures, especially for extremely large events (Kanamori, 1978). For earthquakes with smaller fault ruptures, the moment magnitude generally compares well with the surface wave magnitude M_s or the local magnitude M_L (Kanamori, 1978). The moment magnitude is defined in terms of the seismic moment M_o:

$$M_w = (\log M_o / 1.5) - 10.7 \qquad (3\text{-}1)$$

where M_o is expressed in dyne cm. The seismic moment is based on elastic dislocation theory and represents the deformation at the source of the earthquake:

$$M_o = u\ S\ D \qquad (3\text{-}2)$$

where u is the rigidity of the ruptured material, S is the surface area of the fault and D is the average displacement of the fault.

3.2.1.2 Distance to seismic energy source or nearest fault rupture - We will use a definition of distance to the seismic energy source similar to that given by Joyner and Boore, 1981, 1988. Joyner and Boore define the distance to the source as: "the closest distance to the vertical projection of the rupture on the surface of the earth (Joyner and Boore 1988)." We will define the distance to the source as the horizontal distance from the site to the nearest bound of the zone of seismic energy release projected to the ground surface.

3.2.1.3 Maximum acceleration at the site - Where a strong ground motion accelerometer was located at or near a site, the instrumental peak horizontal acceleration will be tabulated. For those sites without instrumentation, the relationship developed by Joyner and Boore (1981) is used to estimate peak acceleration:

$$\log A = -1.02 + 0.249\, M_w - \log r - 0.00255r + 0.26P \qquad (3\text{-}3)$$

where A is the peak horizontal acceleration on rock or stiff soil given as a decimal fraction of gravity, g, M_w is moment magnitude and P is a probability term that is equal to zero for a 50 percent probability that the predicted value will not be exceeded during an event and one for an 84 percent probability that the predicted value will not be exceeded. We chose a 50 percent probability for this study, thus, the probability term in equation 3-3 was set to zero. The distance factor r is given by:

$$r = (d^2 + h^2) \qquad (3\text{-}4)$$

where d is the closest distance, in km, from the recording site to the surface projection of the fault rupture. Joyner and Boore determined that h equals 4.0 km for shallow earthquakes.

3.2.1.4 Duration of strong ground motion

Page et al., 1972, used the interval in seconds between the first horizontal 0.05 g peak to the last 0.05 g peak to define the duration of strong ground motion. Based on limited data, they presented a table of expected duration versus magnitude. However, this relationship is unrefined and is good only for sites within a 3-5 km of the source.

VanMarcke and Lai, 1980, defined the duration of the earthquake as a function of the maximum ground acceleration and the integral over time of the squared accelerations:

$$s_o = 7.5\ I_o / \ a\ max^2 \qquad (3\text{-}5)$$

where s_o is strong motion duration in seconds, I_o is the integral of the squared accelerations, and a_{max} is the maximum ground acceleration. They have tabulated values of magnitude, distance and strong motion duration for 70 strong ground motion sets (2 components per set) in California. However, no empirical magnitude-distance-duration relationship was given by Vanmarcke and Lai.

Krinitzsky and Chang, 1988b, defined the duration of strong ground motion as the bracketed time that site accelerations equal or exceed 0.05 g. They presented an empirical equation for duration of strong ground motion at soft sites:

$$\log D = -2.06 + 0.43M + 0.60 \log(r/10) \qquad (3\text{-}6)$$

where D is the bracketed duration in seconds, M is the Richter magnitude and r is the focal distance in kilometers. Krinitzsky and Chang, 1988b, report that M, the Richter magnitude, is equivalent to M_w for M up to 8.3 and to M_L for M below 5.9, and to M_s for M at 5.9 to 8.0.

We will use equation 3-6 to estimate the duration of strong ground motion for sites were no accelerogram exists. Otherwise, the bracketed time that the site accelerations equal or exceed 0.05g will be reported.

3.2.2 Geological and Stratigraphic Factors

3.2.2.1 Age of sediment - The sediment age of the liquefied layer is expressed in years before present. If the layer has been dated by C^{14} or other procedures, that age is given. If not, the geological epoch is given.

3.2.2.2 Mode of Deposition - Most sands that have liquefied were laid down as fluvial deposits. The type of deposit (braided stream, point bar, channel deposit, etc.) is described.

3.2.2.3 Total Thickness of the Unconsolidated Sediments - Unconsolidated sediments are sediments that have not be appreciably cemented or lithified. The total depth of unconsolidated sediments is reported in feet.

3.2.2.4 Horizontal Variation of Soil in Profile - Facies changes are lateral changes in the soil composition or texture resulting from horizontal changes in the sedimentary depositional regime. Typically lenses of sands, silts and clay intertongue in natural deposits. These lateral changes affect the extent of the liquefied zone and displacement of the lateral spread. Important facies changes are noted in the geological description of the sites found in the tabulated information (Bartlett and Youd, 1989a).

3.2.2.5 Depth to Groundwater - The depth to free ground water is tabulated in feet.

3.2.2.6 Ground Slope - The ground slope of the lateral spread is reported in percent. Hamada et al., 1986, in their study of lateral displacements in Japan, concluded that horizontal displacement correlated best with the larger value of: 1) the ground slope or 2) the slope of the base of the liquefied zone (Figure 8). For many sites reviewed by this study (except for the Japanese data and some well documented U.S. sites), the number of borings is insufficient to construct a complete cross section of the liquefied zone across the lateral spread. Therefore, the slope of the base of the liquefied zone could not be determined. This study differs from that of Hamada et al., and reports only the value for the ground slope. Hamada et al., 1986, also steepened the ground slope into the river channel for cases where a channel was present (Figure 7). We will also steepen our measurement of the ground slope into the channel when a channel is present.

3.2.2.7 Proximity to free face - A free face is any abrupt topographical depression such as escarpment, stream channel, canal or road cut etc. Many lateral spreads displace downslope towards or into a free face. For example, lateral spreading of the river banks toward the channel during the 1964 Niigata earthquake appreciably decreased the widths of the rivers. Narrowing of stream channels during the 1964 Alaskan earthquake compressed the rails and superstructures of numerous railroad bridges.

The height of the free face and the horizontal distance from the site to the free face should affect displacement. Unfortunately, many of the case

studies do not provide sufficient documentation to determine the height of the free face. If a free face is considered to have influenced the displacement, the horizontal distance from the point were the displacement was measured to the free face is reported in feet.

3.2.2.8 Thickness of the Layers - The thicknesses of the layers in the profile are reported in feet. The appendix contains the standard penetration and cone penetration data for the 111 borings studied. Layer boundaries are marked with a "B" on the bore log summary sheets. Blow counts are marked with a "N". Cross sections, when provided in the original study, are also included.

3.2.2.9 Thickness of Liquefied Zone - The thickness of the liquefied zone was calculated for each site. Where two or more subzones liquefied, the tabulated thickness is the sum of their thicknesses.

Two techniques are used to determine the thickness of the liquefied zone: the simplified procedure proposed by Seed and Idriss and their colleagues (1971, 1982, NRC 1985, Seed et al., 1986a) and Liao's modifications to the simplified procedure (Liao, 1986).

3.2.2.9.1 Thickness of the Liquefied Zone from the Simplified Procedure - The simplified procedure (Seed et al., 1971, 1982, 1983, NRC 1985) has gained wide acceptance and is used to calculated the thickness of the liquefied zone. For a particular soil layer, the simplified procedure compares the cyclic stress ratio generated by the earthquake (CSRQ) to the cyclic stress ratio required to generate liquefaction in the soil (CSRL). The latter ratio (CSRL) is

calculated from reported blow counts and other soil properties. If the calculated CSRQ for a given earthquake exceeds the calculated CSRL, that soil is assumed to have liquefied. The thickness of the liquefied zone was estimated by summing the thickness of the subzone(s) in which CSRQ exceeds CSRL.

From laboratory cyclic shear test, Seed and Idriss, 1982, 1983 defined the average cyclic shear stress developed on a horizontal plane during cyclic loading as s_h, and the initial vertical effective stress as r_o'. They note that the average shear stress induced on the soil by an earthquake is:

$$s_h = 0.65\ (a_{max}/g) * r_o * r_d \qquad (3\text{-}7)$$

where a_{max} is the maximum ground acceleration, g is the acceleration of gravity, r_o is the in-situ vertical stress in lb/ft^2 and r_d is a stress reduction factor. The earthquake induced stress is then divide by the in-situ effective vertical stress to define the earthquake induced cyclic stress ratio:

$$CSRQ = s_h/r_o' = 0.65\ (a_{max}/g) * r_d/r_o' * r_d \qquad (3\text{-}8)$$

The stress reduction factor, r_d, which is a function of depth, z, in feet is:

$$r_d = 1 - 0.025092\ z \qquad (3\text{-}9)$$

for z \ 30 ft and

$$r_d = 1.174 - 0.090528\ z \qquad (3\text{-}10)$$

for z > 30 ft (Liao, 1986).

The soil's resistance to liquefaction is determined from the standard penetration resistance of the soil and other soil properties. The measured blow counts, N, are normalized to an effective stress of 1 ton/sq. ft. using the equations:

$$N_1 = C_N * N \qquad (3\text{-}11)$$

where N_1 is the normalized blow count and C_N is an overburden correction factor. C_N is calculated from:

$$C_N = (1/r_o')^{1/2} \qquad (3\text{-}12)$$

where r_o' is expressed in tons/sq. ft (NRC, 1985). N_1 is then corrected for the measured energy ratio of the hammer to a standard hammer energy ratio of 60 percent. The hammer correction is as follows:

$$(N_1)_{60} = N/60 * ER_m \qquad (3\text{-}13)$$

where $(N_1)_{60}$ is the final corrected blow count and ER_m is the measured energy efficiency ratio of the hammer expressed in percent. Typically, safety hammers using a rope and pulley release have an energy ratio of about 60 percent and Donut hammers using a rope and pulley release have an energy ratio of about 45 percent (NRC, 1985).

The resistance of the soil to liquefaction is determined from a standard curve develop by Seed et al. (from NRC 1985, see Figure 5, valid only for earthquakes of M = 7.5). The CSRL values read from this curve have been digitized by us. Table 3 gives the digitized values for M = 7.5 and a fines content of less than or equal to 5 percent.

TABLE 3

Minimum Cyclic Stress Ratio Required to Cause Liquefaction (CSRL) for Various $(N_1)_{60}$ Values (7.5 M, Fines content less than or equal to 5 percent)

$(N_1)_{60}$	CSRL	$(N_1)_{60}$	CSRL	$(N_1)_{60}$	CSRL
0	0.000	11	0.122	21	0.234
1	0.011	12	0.133	22	0.248
2	0.022	13	0.144	23	0.262
3	0.033	14	0.155	24	0.278
4	0.044	15	0.167	25	0.296
5	0.056	16	0.178	26	0.316
6	0.067	17	0.189	27	0.339
7	0.078	18	0.200	28	0.367
8	0.089	19	0.211	29	0.405
9	0.100	20	0.222	30	0.500
10	0.111				

When the cyclic stress ratio induced by an earthquake, CSRQ, is greater than the cyclic stress ratio required to cause liquefaction, CSRL, the soil at that depth is marked as liquefiable (marked with an asterisk on bore log sheet in the appendix). If CSRL is greater than CSRQ, the soil is considered resistant to liquefaction.

The CSRL curve given in Figure 5 (Seed et al., 1983) and digitized in Table 3 is valid only for M = 7.5 earthquakes and must be adjusted for other earthquake magnitudes (Figure 10). This curve is adjusted by multiplying the values in Table 3 by a magnitude sealing or normalization factor, MNF:

$$MNF = 0.032\ M^2 - 0.631\ M + 3.9334 \qquad (3\text{-}14)$$

where M is the earthquake magnitude (Liao, 1986).

Seed and Idriss, 1982, found that soils with significant fines contents should generally <u>not</u> liquefy. They gave the following criteria for non-liquefiable soils.

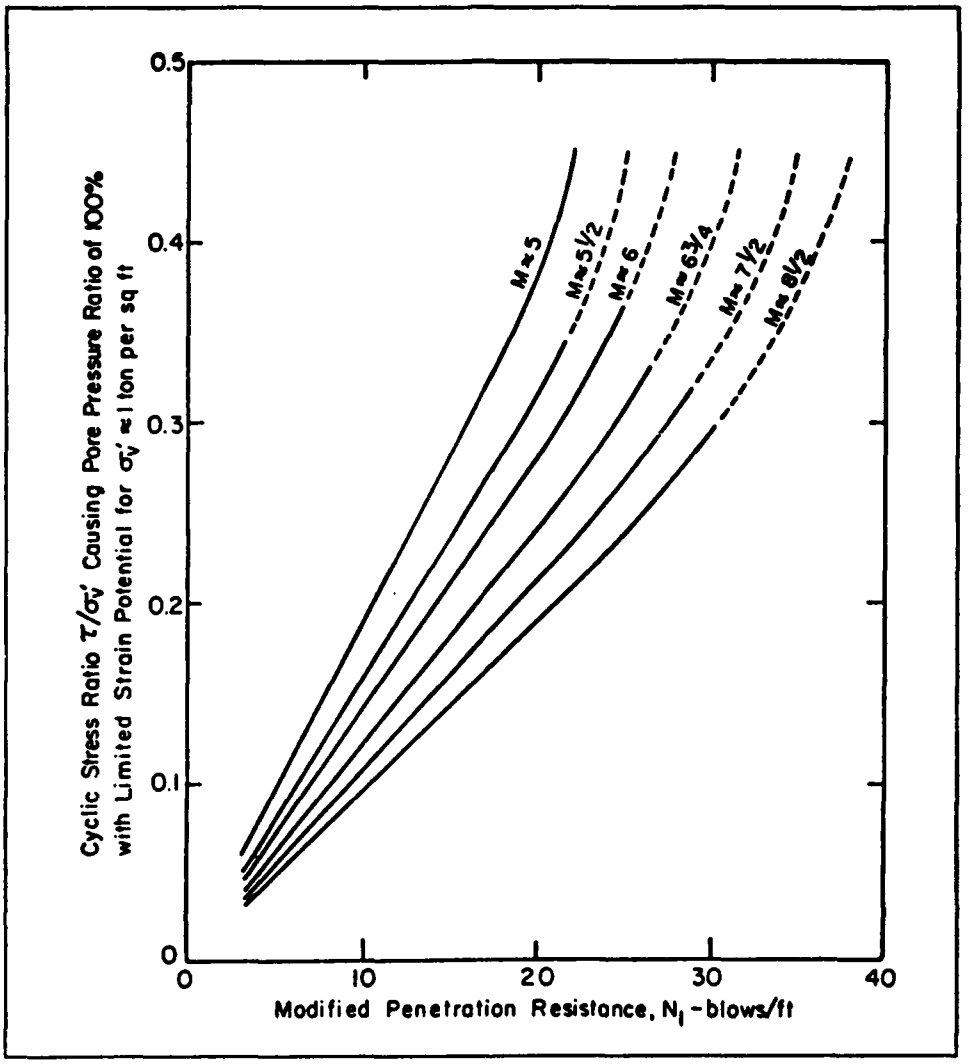

Figure 10 Chart for Evaluation of Liquefaction Potential for Sands for Earthquakes of Different Magnitudes (NRC, 1985).

1) Soils that have 15% or greater clay content (percent finer than 0.005 mm.)

2) Soils that have a liquid limit greater than 35.

3) Soils that have a water content less than 0.9 times the liquid limit.

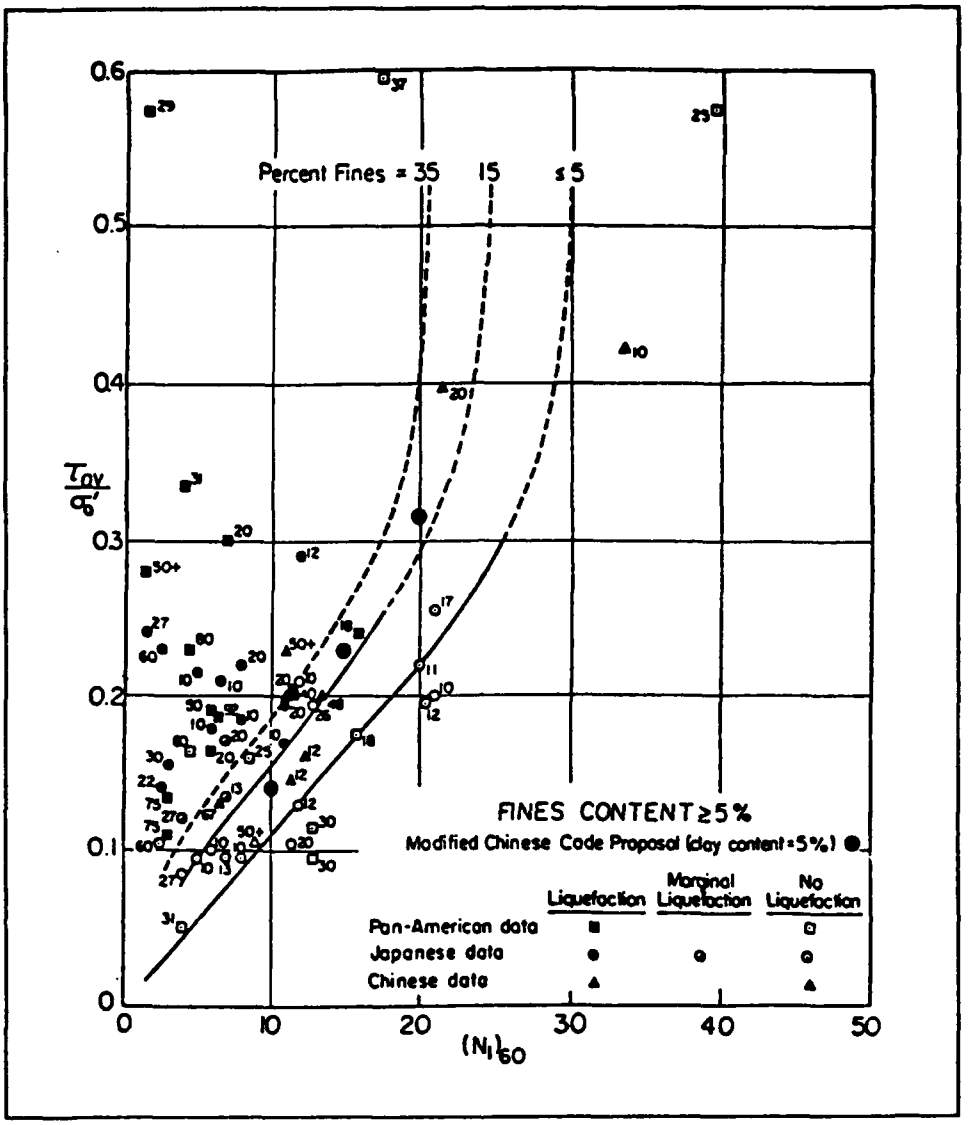

Figure 11 Relationship Between Stress Ratio Causing Liquefaction and $(N_1)_{60}$ Values for Silty Sands for Magnitude 7.5 Earthquakes (NRC, 1985).

For a given N_1, soils with high fines contents are less susceptible to liquefaction than clean sands (NRC, 1985, Liao, 1986). The CSRL curve must be adjusted for sands with fines contents greater than 5 percent (see Figure 11, % fines = percent finer than 0.075mm). Factors used to correct the CSRL curve for fines contents of 15 percent and 35 percent are listed in Table 4. Linear

TABLE 4

FINES CORRECTION FACTORS FOR CSRL CURVES FOR 15 % AND 35 %

CSRL	FCF 15%	FCF 35%	CSRL	FCF 15%	FCF 35%	CSRL	FCF 15%	FCF 35%
0.00	1.64	1.99	0.10	1.50	1.77	0.20	1.34	1.63
0.01	1.64	1.99	0.11	1.45	1.74	0.21	1.34	1.69
0.02	1.64	1.99	0.12	1.40	1.69	0.22	1.35	1.76
0.03	1.64	1.99	0.13	1.39	1.68	0.23	1.36	2.02
0.04	1.64	1.99	0.14	1.38	1.65	0.24	1.38	----
0.05	1.64	1.99	0.15	1.37	1.63	0.25	1.42	----
0.06	1.64	1.99	0.16	1.36	1.61	0.26	1.45	----
0.07	1.64	1.99	0.17	1.35	1.61	0.27	1.49	----
0.08	1.55	1.89	0.18	1.35	1.59	0.28	1.55	----
0.09	1.51	1.83	0.19	1.35	1.60	0.29	1.72	----

* The 35% FCF for CSRL > 0.19 is undefined.
** The 15% FCF for CSRL > 0.29 is undefined (see Figure 11).

interpolation is used to estimate correction factors for fines contents between 5 and 35 percent (the fines correction factor for fines contents of five percent or less is 1.0 for all values of CSRL).

There are no defined guidelines for soils that have a fines content exceeding thirty-five percent and a clay content below 15 percent. These soils may also be susceptible to liquefaction. Because of the lack of a better criterion, we used the correction factor for soils with 35 percent fines for all soils with fines contents greater than 35 percent.

3.2.2.9.2 Thickness of the Liquefied Zone from Liao's Modifications to the Simplified Procedure - Liao, 1986 analyzed 278 sites with liquefaction or non-liquefaction to develop a best fit, probabilistic model to predict liquefaction. In Liao's procedure, CSRQ is normalized for the magnitude of the earthquake instead of CSRL:

$$CSRQN = CSRQ/MNF \qquad (3\text{-}15)$$

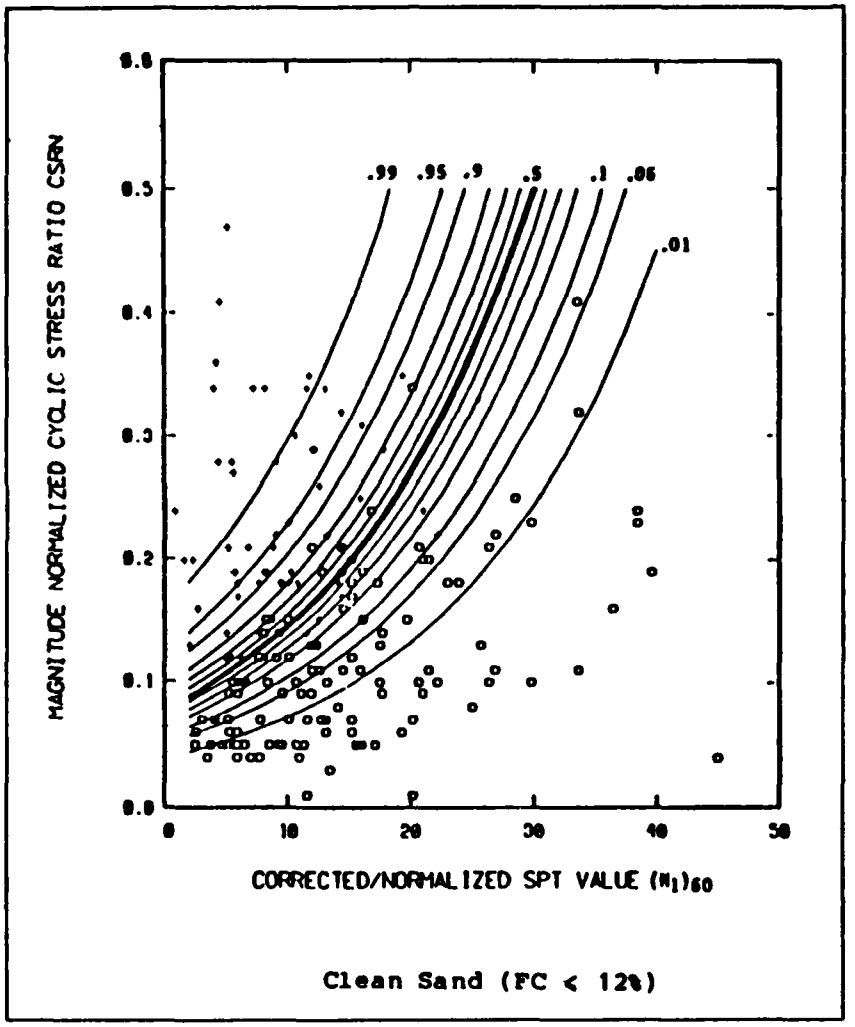

Figure 12 Contours of Equal Probability of Liquefaction for Clean Sands (Liao, 1986).

where CSRQN is the normalized cyclic stress ratio generated by the earthquake, CSRQ is calculated from eq. 3-8, and MNF, a magnitude normalization factor is calculated from eq. 3-14. If the calculated CSRQN for the given earthquake exceeds the calculated CSRL, that soil is assumed to have liquefied.

Liao formulated a set of probability curves to calculate CSRL (Figure 12). For our liquefaction analysis, we choose the 50 percent probability curve. The value of the CSRL for fines contents $\leq$ 12% is:

$$CSRL = EXP((0.39760((N_1)_{60}) - 16.447)/6.4603) \qquad (3\text{-}16)$$

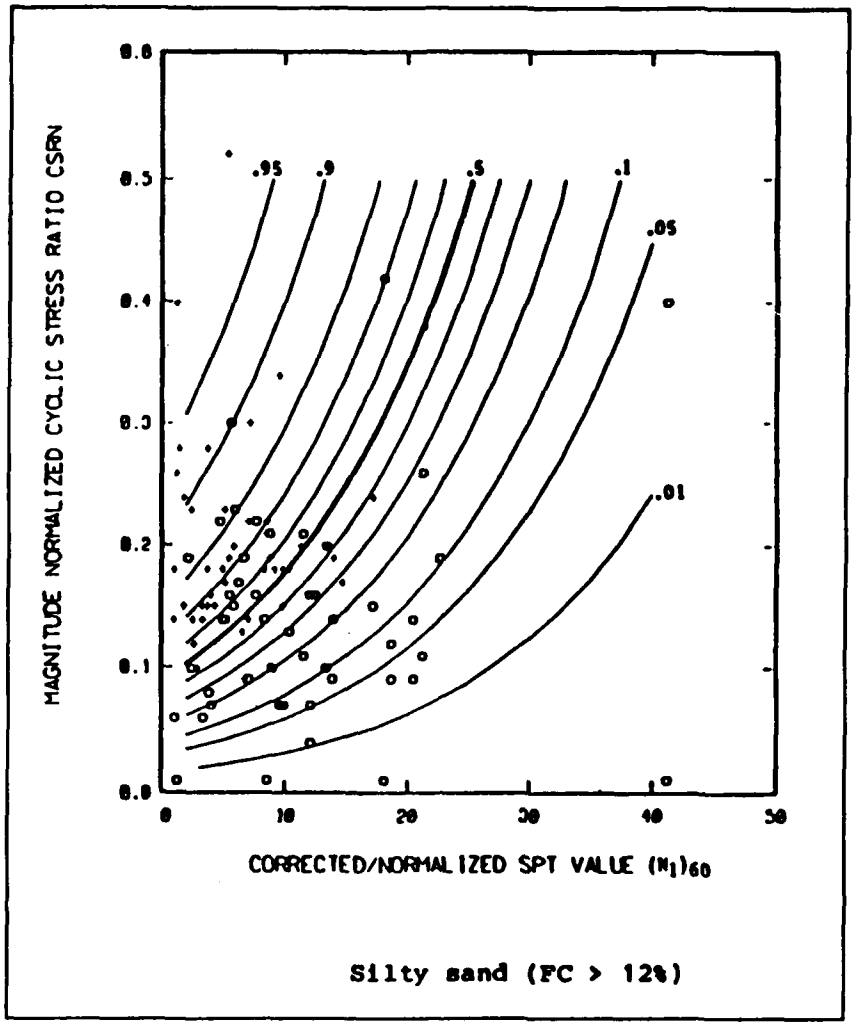

Figure 13 Contours of Equal Probability of Liquefaction for Silty Sand (Liao, 1986).

where $(N_1)_{60}$ is the normalized blow count. The value of the CSRL for fines contents > 12% is (Figure 13):

$$CSRL = EXP((0.18190((N_1)_{60}) - 6.4831)/2.6854). \quad (3\text{-}17)$$

3.2.2.9.3 A Computer Program to Determine the Thickness of the Liquefied Zone using the Simplified Procedure and Liao's Modifications to the Simplified Procedure - A computer program has been written in dBase III to perform the liquefaction analysis. DBase was chosen because of its database capabilities

which allow it to store numerous processed records and make further calculations on those records. The dBase source code and databases for the liquefaction analysis program are available upon request. If a copy of the dBase III interpreter is unavailable to the reader, a compiled but not thoroughly tested version of the program is also available.

The liquefaction analysis program evaluates the soil profile at 0.33 foot increments for liquefaction susceptibility. For this analysis, modified blow count values are linearly interpolated between measured blow counts. A factor of safety, FS, is calculated for each 0.33 foot increment where:

$$FS = CSRL/CSRQ. \qquad (3\text{-}18)$$

A factor of safety less than one indicates that the soil liquefied; a factor of safety greater than one indicates that it did not liquefy.

We define a term called the liquefaction potential of the soil, L, as:

$$L = \text{SUMMATION } (1 - FS)\, dz \qquad (3\text{-}19)$$

where dz is the change in vertical depth in feet. This is comparable to the index of liquefaction potential, P_L, defined by Hamada et al., 1986, except that FS is determined from the simplified procedure or Liao's 50 percent probability curve and the summation is evaluated for the entire depth of the profile and is not terminated at 20 meters. (The W term introduced by Hamada, et al., 1986, which limits the index of liquefaction potential, P_L, to a maximum value of 100 and a minimum value of 0 was not used). The liquefaction potential, L, for any given profile will increase as factors of safety decrease or the thickness of the liquefied zone increases. Calculated values of L for each site are tabulated in the appendix.

3.2.2.10 Low and Average Blow Count for the Liquefied Zone - There remains

some uncertainty about how shear deformation is distributed in the liquefied zone. In order to discover if a low blow count or zone of low blow counts control the amount of horizontal displacement, the low blow count for each boring that occurs in a potentially liquefiable sediment is tabulated on the measurements for regression analysis sheet in the appendix. Soils that have 15% or less clay content (percent passing 0.005 mm), and that have a liquid limit less than 35 and that have a water content greater than 0.9 x liquid limit are defined as potentially liquefiable sediment (Seed and Idriss, 1982). Additionally, the low $(N_1)_{60}$ value corresponding to the low blow count is tabulated (see measurements for regression analysis sheet, appendix). An average blow count and an average $(N_1)_{60}$ value for the liquefied zone is also calculated and recorded. Similarly an average $(N_1)_{60}$ value minus one standard deviation will be calculated and recorded. Statistical models using each of the blow count measures (i.e., low $(N_1)_{60}$ average $(N_1)_{60}$ and average $(N_1)_{60}$ minus one standard deviation values) should allow an evaluation of which predictors best estimates horizontal ground failure displacement.

3.2.2.11 CPT Data - The liquefaction analysis program has the capability to convert CPT tip resistances to SPT blow counts using the q_c/N_{60} curve developed by Seed and de Alba, 1986a, and extended to larger grain sizes by Andrus and Youd, 1989. Three lines were used to match the curve (see Figure 14):

$$q_c/N_{60} = 1.5 \log D_{50} + 5 \qquad (3\text{-}20)$$

for $0.01\text{mm} < D_{50} < 1\text{mm}$,

$$q_c/N_{60} = 2.3 \log D_{50} + 5 \qquad (3\text{-}21)$$

for $1\text{mm} < D_{50} < 10\text{mm}$ and

$$q_c/N60 = 5.3 \log D_{50} + 2 \qquad (3\text{-}22)$$

for D_{50} > 10mm, where q_c is in tons/sq. foot.

3.2.2.12 Depth to Top of Liquefied Zone - The depth to the top of the liquefied zone is recorded for each boring (see appendix, Measurement for Regression Analysis sheet). In no instance was the top of the liquefied zone allowed to rise above the depth of the water table.

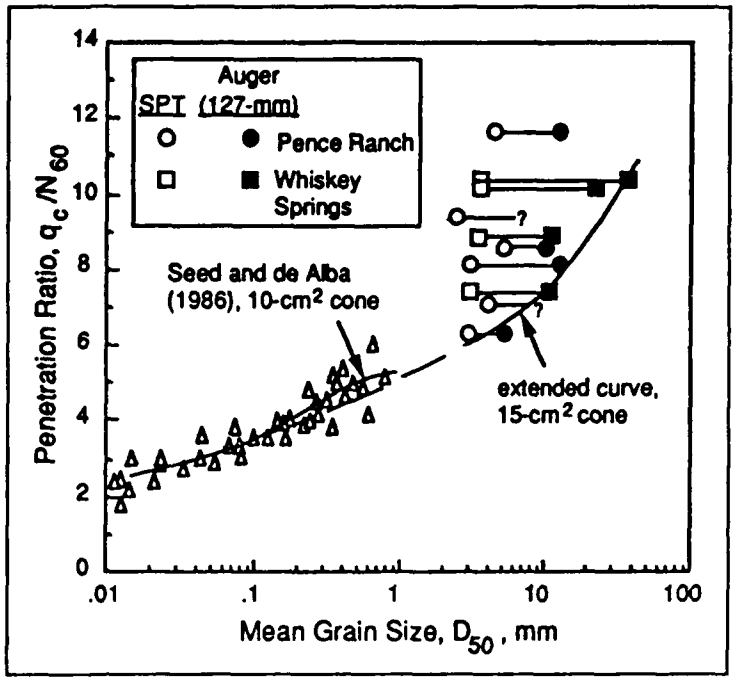

Figure 14 Modified Relationship Between q_c/N_{60} and Mean Grain Size (after Andrus and Youd, 1989).

3.2.2.13 Depth to Lowest $(N_1)_{60}$ - The depth to the low blow count that occurs in a potentially liquefiable sediment is recorded for each boring (see appendix).

3.2.2.14 Confinement of the Liquefied Layer by Less Permeable Layers - The presence of a less permeable layer above and below a liquefied zone retards the migration of pore water which could lengthen the time a liquefied condition exists and increase generated displacement. If confinement of the layer is appreciable, pore pressure build up is expedited and the liquefaction is reach more rapidly. Confinement of the liquified zone is noted in the appendix on the Measurements for Regression Analysis sheet.

3.2.2.15 Areal Extent of Failure - The surface areal extent of the lateral spread are recorded in square feet when documented in the original field study. This measurement is seldom given, however.

3.2.2.16 Horizontal Displacement - The horizontal displacement of the lateral spread are reported in inches. For the regression analysis, each boring is assigned a displacement that occurred at or near that boring.

3.2.3 Soil Factors

3.2.3.1 Soil Description - The Unified Classification System is used as a soil descriptor when it is reported. Otherwise, the descriptive terms (e.g. silty sand) given by the original authors is recorded.

3.2.3.2 Liquid Limit, Plastic Limit and Plastic Index - Atterberg limits for the soil profile, including the liquefied zone, are include on the soil logs when reported by the original investigators.

3.2.3.3 Percentage of Fines and Clay - The fines content is defined as that fraction of the particles by weight finer than 0.075mm. The clay content is defined as that fraction of particles finer than 0.005mm. (This definition of clay sizes varies slightly from the normal definition of 0.002mm, but the 0.005mm demarcation was used by Seed and Idriss, 1982, to divide potentially liquefiable soils from nonliquefiable soils).

The percentage of fines and clay are required measurements for liquefaction analyses. In many site investigations these percents are not

reported. The follow table (see Table 5) was used to estimate the fines and clay percentages for sites that lacked sieve analyses. This table was compiled using grain size data and soil descriptions from Wildlife and Whiskey Springs. Complete grain size and soil descriptions were documented an reported for a wide range of soil types at these two liquefactions sites.

TABLE 5

Estimated Fines and Clay Contents for Various Soil Descriptions
(Grain Size Data taken from Wildlife and Whiskey Springs)

Soil Description	Estimated % fines	Estimated % clay
gravel	5	0
sandy gravel	10	5
silty gravel	25	10
clayey gravel	50	20
silty clayey gravel	40	20
clayey silty gravel	35	15
silty sandy gravel	15	10
sandy silty gravel	25	10
sand	5	0
silty sand	25	5
clayey sand	35	20
silty clay sand	30	20
clayey silty sand	30	20
sand & silt	45	10
clayey sand & silt	60	30
silt	90	15
sandy silt	75	10
clayey silt	99	35
sandy clayey silt	85	25
gravelly silt	75	10
clay	95	80
silty clay	95	60
sandy clay	75	50
silty sandy clay	85	55

CHAPTER 4: FORMULATION AND EVALUATION OF FUNCTIONAL REGRESSION MODELS

4.1 Introduction

Studies summarized in Chapter 2 by Newmark, 1965, Ishihara, 1985, Hamada et al., 1986 and Youd and Perkins 1987 have shown that several seismic, topographic, geological and soil factors affect horizontal ground displacement. We have tabulated many of these factors for U.S. and Japanese case studies of liquefaction sites (see appendix to this report). Chapter 3 outlines and defines the many data that we have collected. It also gives the procedures and techniques used to estimate measurements that were missing from the reported case studies.

We now proceed to formulate functional regression models from these tabulated factors. Formulation of a functional regression models means that the researcher uses his or her knowledge of the functional form of the relationship between the independent and dependent variable to assist in expressing the form of the model. For example, it is generally proven that seismic effects such as intensity of ground shaking decrease logarithmically with increasing distance from the seismic source. Thus, a functional regression form to predict intensity of ground shaking using distance from the seismic source would be:

$$y = 1/x^a$$

where y represents some measure of intensity of ground shaking and x is the distance from the seismic source and a is empirically determined constant. The function is typically linearized by taking the log of both sides before the regression analysis is performed:

$$\log y = - a \log x.$$

The following sections define the proposed functional relationship between the independent and dependent variables for the factors we have tabulated. Later, these factors are combined to formulate functional regression models. We conclude by preforming correlation and regression analyses on our proposed models and compare their performance with existing models.

4.2 Seismic Factors

4.2.1 Acceleration and Duration

Horizontal ground shaking induces liquefaction and generates inertial forces that may cause horizontal displacement of decoupled surface layers overlying the liquefied soil. Theoretically, larger horizontal ground accelerations should produce larger horizontal displacements.

Longer durations of ground shaking should increase the extent of liquefaction in the layer, maintain a liquefied condition over a longer period of time and increase the time available for downslope movement under a combination of earthquake and gravitational forces. Youd and Perkins, 1987, proposed that horizontal ground displacement is a function of acceleration and duration:

$$X = f(A, D) \qquad (4\text{-}1)$$

where X is the horizontal ground displacement, A is the horizontal ground acceleration, and D is the duration of the strong ground motion. Equation 4-1 written in terms of the factors measured in this study is:

$$X = f(a_{max}\ D) \qquad (4\text{-}2)$$

where a_{max} is the peak horizontal ground acceleration and D is the duration.

4.2.2 Magnitude and Distance

Horizontal ground displacement should increase with earthquake magnitude because both a_{max} and D generally increase with earthquake magnitude. Horizontal ground displacement should also decrease with distance from the energy source because of the attenuation of ground acceleration with distance from the energy source.

Youd and Perkins, 1987, suggested a relationship for horizontal ground displacement in terms of magnitude and distance. In general terms this relationship is:

$$X = f(M_w 1/R) \qquad (4\text{-}3)$$

where M_w is the moment magnitude and R is the horizontal distance from the site to the nearest bound of the seismic energy release.

4.3 Layer Factors

4.3.1 Thickness of the liquefied zone and zone of low $(N_1)_{60}$ within the liquefied zone

It is not clear whether shear deformation is distributed across the entire liquefied zone or limited to a subzone zone of lower blow counts within the liquefied zone or concentrated along a definite shear plane within the layer. Hamada et al., 1986, after studying horizontal displacement from the Niigata and Nihonkai-Chubu earthquakes, postulated that: "displacements are surmised to be caused not by sliding on only one particular slip plane in the soil layer, but by shearing deformation throughout the liquefied layer." Some observational evidence supports this supposition. Piles that have been

fractured by lateral spread displacement have generally been fractured and deformed at multiple points indicating a zone of displacement rather than a single point as might be expected for displacement across a single plane (Hamada, et al., 1986).

In general, the relationship between horizontal displacement and the thickness of the liquefied zone should be:

$$X = f(t) \qquad (4\text{-}4)$$

where t is the thickness of the liquefied zone. Two estimates of the thickness of the liquefied zone were calculated for this study, t_s using the simplified procedure of Seed et al. 1982, 1983, and t_l using the modifications to that procedure proposed by Liao. Thus

$$X = f(t_s) \qquad (4\text{-}5)$$

or

$$X = f(t_l) \qquad (4\text{-}6)$$

There is some evidence that a subzone of low blow counts within liquefied layer may control displacement. Andrus and Youd, 1987, concluded that shearing within silty gravel at a lateral spread near Whiskey Springs, Idaho was primarily within a 5 ft thick sublayer with low blow counts (N = 5 - 10) located immediately beneath the water table. An underlying layer with higher blow counts (10-20) was also susceptible to liquefaction but apparently did not deform. Additionally, in areas where the lower blow-count zone was above the water table, no appreciable displacement occurred even though liquefaction analysis shows a considerable portion of the underlying sediment should have liquefied. These observations suggest a model that incorporates a low blow count or counts within the liquefied zone as a key factor to model the shear strength in a weaker zone where most of the deformation may be

occurring. In general, the relationship between the horizontal displacement and the $(N_1)_{60}$ value should be:

$$X = f(1/N) \qquad (4\text{-}7)$$

where N could be either the low $(N_1)_{60}$ value, the average $(N_1)_{60}$ value, or the average $(N_1)_{60}$ value minus one standard deviation in the liquefied zone.

4.3.2 Liquefaction Potential

The liquefaction potential, L, defined in section 3.2.2.9.3, for any given profile increases as factor of safety against liquefaction decreases and as the thickness of the liquefied zone increases. The relationship between X and L should be:

$$X = f(L). \qquad (4\text{-}8)$$

Again, both the CSRL curves of Seed et al, (1971, 1982, 1983, NRC 1985) and Liao, 1986, were used to calculate the L. Both results are use in the analyses herein. The L calculated from the curves of Seed et al. is given the symbol L_s and that calculated from Liao's curves is given the symbol L_l.

4.3.3 Depth to liquefied zone and to low $(N_1)_{60}$ value

Ishihara, 1985, found that surface manifestations of liquefaction are dependent on both the thickness of overlying unliquefied sediment and the thickness of the liquefied layer. To combine the factors, we define a thickness ratio, T, as the ratio of the thickness of the liquefied zone, t, to the depth of the top of the liquefied zone, z:

$$T = t/z. \qquad (4\text{-}9)$$

As previously noted, the thickness of the liquefied zone, t, can be determined by the simplified procedure of Seed and et al., or Liao's 50 percent

probability curve, thus:

$$T_s = t_s/z_s \qquad (4\text{-}10)$$

and

$$T_l = t_l/z_l \qquad (4\text{-}11)$$

In general, the following relationship should exist between the horizontal displacement and the thickness ratio:

$$X = f(T). \qquad (4\text{-}12)$$

However, if a zone of low blow counts within the liquefied layer is controlling displacement, it might be more appropriate to use the depth to the low $(N_1)_{60}$ value as the depth factor. Thus,

$$X = f(1/z_{60}) \qquad (4\text{-}13)$$

where z_{60} is the depth to the low $(N_1)_{60}$ value.

4.4 Topographical Factors

4.4.1 Ground Slope and Free Face

Once a layer has liquefied, the component of gravity acting parallel to the ground slope becomes an additional driving force producing downslope displacement. Hamada, et al., 1986, found that horizontal displacement correlated with the ground slope or the gradient of the base of the liquefied zone. For most of the case studies we compiled, there is inadequate subsurface data to define the slope of base of the liquefied zone. Therefore, we use the ground slope in our analyses. For cases where a free face is present, we steepened our estimate of the ground slope to the bottom of the channel or depression. The general relationship of horizontal displacement and ground slope, *S*, is:

$$X = f(S) \qquad (4\text{-}14)$$

Where a free face is near, the liquefied sediments may not be as constrained as in the absence of the free face, and larger displacement may occur. We tabulated the distance, X, from points where displacements were measured to the nearest free face and include it as a predictor variable in our models. In general, the relationship between horizontal displacement and the distance to the free face is:

$$X = f(1/F) \qquad (4\text{-}15)$$

4.5 Preliminary Functional Regression Models

The models fashioned below include seismic factors, layer and soil factors and topographical factors. In general, they may be classified into two general groups based on the seismic factors: 1) acceleration - duration models and 2) magnitude - distance models. The topographical factors (i. e. ground slope and distance to free face) are common to all models. However, the layer and soil factors (thickness/depth, liquefaction potential, $(N_1)_{60}$ depth), are interchanged from model to model. This will allow us to test which layer and soil factors are better predictors of ground displacement while controlling the influence of the seismic and topographical factors. The general forms of the models we tested are presented below.

MODELS TESTED

Acceleration Duration Thickness/Depth Slope Free Face Model

$$\ln X = y_o + b \ln a_{max} + c \ln D + d \ln T + e \ln S + f \ln F \quad (4\text{-}16)$$

Acceleration Duration Liquefaction Potential Slope Free Face Model

$$\ln X = y_o + b \ln a_{max} + c \ln D + d \ln L + e \ln S + f \ln F \quad (4\text{-}17)$$

Acceleration Duration $(N_1)_{60}$ Depth Slope Free Face Model

$$\ln X = y_o + b \ln a_{max} + c \ln D + d \ln N + e \ln z + f \ln S + g \ln F \quad (4\text{-}18)$$

Magnitude Distance Thickness/Depth Slope Free Face Model

$$\ln X = y_o + b M_o + c \ln R + d \ln T + e \ln S + f \ln F \quad (4\text{-}19)$$

Magnitude Distance Liquefaction Potential Slope Free Face Model

$$\ln X = y_o + b M_o + \ln R + \ln N + \ln D + \ln S + \ln F \quad (4\text{-}20)$$

Magnitude Distance $(N_1)_{60}$ Depth Slope Free Face Model

$$\ln X = y_o + b M_o + c \ln R + d \ln N + e \ln z + f \ln S + g \ln F \quad (4\text{-}21)$$

where y_o, b, c, d, e, f, g are regression constants.

4.6 Preliminary Evaluation of Our Regression Models

To see if these functional empirical models for predicting ground displacements have any significance, we conducted preliminary analyses using the data complied in the appendix.

4.6.1 Pairing of the Dependent Variable with the Independent Variables

Two methods of pairing the independent variables with the dependent variable were used to analyze the models listed above. In the first pairing scheme, a boring log and the corresponding layer and topographical

measurements (i.e., independent variables, e.g. thickness of the liquefied zone, depth to liquefied zone, slope of ground surface at boring, distance from boring to free face, etc.) were paired with a unique horizontal displacement (dependent variable). Two pairing situations arose which required some interpretation. First, some of the sites had only a few displacement measurements recorded in the vicinity of several drill holes and the proximity of the measured displacements to the individual borings was not clear. Second, in contrast, some sites showed several measured displacements near one boring. For the first set of regression analyses, the following pairing was tried:

1) Each measured displacement at a particular site was paired with the boring closest to the displacement.

2) If only one displacement existed for several borings and the location of the displacement in respect to the borings was uncertain, the boring that had the highest liquefaction potential, L, was paired with the measured displacement.

3) Where several measured displacements were clustered around a boring, the measured displacement nearest to the boring was chosen for pairing with the boring.

4) When the ground slope at the measured displacement was known, this slope was used for pairing with the displacement. If the ground slope at the measured displacement was not recorded, an average ground slope for the failure was determined from cross sections or topographical maps and paired with the measured displacement.

Of the 111 bore hole records tabulated in the appendix, 92 boring - displacement pairs were established. Preliminary regression analyses performed using these 92 borings - displacement pairs yielded low coefficients of determination, ranging from 0.11 to 0.27 for the various models. The following factors may have contributed to the poor predictions from the first set of analyses:

1) The pairing of a measured displacement with a boring that best represents the liquefied layer properties for that particular displacement involves some judgement. In cases where only one displacement was recorded for a group of borings, the selection of the boring with the highest liquefaction potential, L, for pairing with the measured displacement may not be a good approach.

2) It is difficult to define the ground slope at a particular boring. Many borings were from bridge investigations and are located at the top of a slope, edge of a stream bank or at the toe of a slope where the slope is abruptly changing. The adjacent topography may have a considerable affect on the ground displacement. Obviously, the slope of a line tangent to the topography at the point in consideration may not represent the influence of adjacent topographical relief.

3) The distance from the measured displacement to the free face was often estimated.

4) Estimation or poor measurement of other predictor variables in the database may have increased the variance and experimental error.

A second method of pairing the independent variables with the dependent variable was used. For the second set of regression analyses performed, data were combined by averaging segments of layer and topographical measurements (e.g., thickness of the liquefied zone, depth to top of the liquefied zone, low $(N_1)_{60}$ value, depth to low $(N_1)_{60}$ etc.) where only one displacement was reported at a site and several borings were available. Likewise, where several displacements were reported for a given cross section, the cross section was divided into segments that appeared to displace as a block (see figures 6 & 7). The displacements were averaged throughout the block and the layer and topographical measurements for that segment were combined (averaged). The averaging of displacements within a block made the distance from the averaged displacement to the free face meaningless so it was excluded from the second analyses.

The averaging of site factors decreased the variability of the predictor variables and not surprisingly the coefficient of determination increased for all models. Model 4-16 gave the best fit to the compiled data set. Overall, our analysis indicates that model 4-16 is statistically significant model at the 99 percent confidence level. However, a relatively low coefficient of determination ($r^2 = 0.34$) indicates that the model is explaining only 34 percent of the variability found in the measured displacements. Therefore, we refrain from reporting the coefficients for model 4-16 until our measurements of the independent variables are refined and better results are obtained.

Additionally our analysis of model 4-16 shows that coefficients for strong motion duration and the thickness of liquefied zone divided by the depth to the top of the zone are significant predictors of displacement at the 95 percent confidence level. However, the acceleration, slope and free face

coefficients were not significant at the same degree of confidence. We do not wish to imply that these factors do not affect ground displacement, but we do suggest that our definition and measurements of these factors needs to be improved by further research.

4.7 Observations and Conclusions about the Empirical Models Tested

We offer the following observations and comments regarding the general performance of all empirical models tested. The results of these are very preliminary and appear to have mixed degrees of statistical and intuitive significance. These observations may change as our database is enlarged and improved. Performance of the models was judged by the strength of the relationship (as indicated by the coefficient of determination) and the correctness of the relationship (e.g. horizontal displacement increasing with slope, horizontal displacement decreasing with distance from the energy source, etc.).

1) Many of the maximum ground accelerations, a_{max} and most of the strong ground motion durations used in the acceleration - duration models were calculated from magnitude - distance attenuation relationships which may not be representative of actual site accelerations and durations. Refinement of the estimates for these factors may produce better predictions from acceleration - duration models. Additionally, models that included acceleration and duration for the seismic predictor variables gave slightly better results than models that used magnitude and distance for the seismic predictor variables. The distance relationship in the magnitude - distance models was wrong in some cases

(these models were predicting slightly increased horizontal displacement with increasing distance from the source of the earthquake). The reasons for this anomaly are unclear. Perhaps the predominance of sites that are 15 miles or less from the zone of energy release is causing horizontal displacement to appear to be somewhat independent of distance. The acceleration - duration models did predict the right relationship (horizontal ground displacement increasing with maximum acceleration and duration of earthquake shaking) in most cases. However, some of the maximum ground accelerations and most of the strong motion durations reported by this study for the sites were calculated from magnitude - distance relationships. This suggests that magnitude - distance models may ultimately perform as well as acceleration - duration models.

2) Preliminary models that used the thickness ratio, T, had higher coefficients of determination than models that use a low $(N_1)_{60}$ average $(N_1)_{60}$ or average $(N_1)_{60}$ minus one standard deviation. It appears that the total thickness of the liquefied zone is better estimator of horizontal ground displacement than any of the various $(N_1)_{60}$ values tested. This suggests that the larger horizontal displacements can be expected where thicker zones of potentially liquefiable sediments exist. For most cases studies, it appears that a zone of low blow counts within the liquefied layer may not influence the horizontal displacement as much as the total thickness of the liquefied zone(s).

3) Models that used the liquefaction potential, L, (see section 3.2.2.9.3), as a predictor variable had lower coefficients of determination than models that used the thickness ratio, T. This observation is comparable to the observation made by Hamada et al., 1986. In their study, the index of liquefaction potential P_L, which is similar to L, did not correlate with horizontal displacement as well as the total thickness of the liquefied zone.

4) Models which used the simplified procedure of Seed et al., 1971, 1982, 1983, NRC 1985, to define the thickness of the liquefied zone yielded slightly higher coefficients of determination than models which used Liao's 50 percent probability curve (Liao, 1986). However, these differences were small and the use of either procedure should give comparable results.

5) The inclusion of ground slope as a predictor variable did not significantly improve the coefficient of determination for most models. However, we do not imply that ground slope does not influence horizontal displacement. The averaging of displacements, layer measurements, and slopes at some sites, as was done for the second set of regression analyses, probably tended to obscure the influence of slope on the amount of horizontal displacement and reduce its correlation with displacement. Additionally, the influence of the free face on horizontal displacement could not be adequately tested by this study. An attempt was made to use a horizontal distance measured from the point of displacement to the free face as a predictor variable. But when

several borings were combined and displacements averaged for a displacement block, as was done for the second set of regression analyses, the horizontal distance to the free face became difficult to define and its local affect on ground displacement was obscured. In order to more adequately model ground displacement near a free face, more research is needed to understand the free face's relationship to ground slope and depth to the liquefied zone and how these factors combine to influence ground displacement.

4.8 Preliminary Evaluation of Hamada et al., 1986 Regression Model

In this section, we report some preliminary tests we have made of on the performance of the regression equation reported by Hamada et al., 1986 (see section 2.5.4) by calculating the coefficient of determination, r^2 for the measured versus predicted displacements for Japanese and U.S. case studies.

From displacements and other data measured at liquefied sites in Niigata, Noshiro and Juvenile Hall during the respective 1964 Niigata, 1983 Nihonkai-Chubu and 1971 San Fernando Earthquakes, Hamada et al., 1986, developed the following regression equation to predict horizontal displacement:

$$D = 0.75\ H^{0.48} S^{0.33} \qquad (4\text{-}22)$$

where D is the horizontal displacement in meters, H is the thickness of the liquefied zone, in meters, determined from the Japanese Code of Bridge Design, and S is the larger of the gradient of the ground surface or the lower boundary face of the liquefied zone in percent.

Hamada et al., 1986, present a scatter plot of observed versus predicted displacements to visually show the performance of their model (see Figure 15).

Those data points that fall near the 45 degree line are closely approximated by the regression equation. The line below the 45 degree line represents a 100 percent over-prediction bound. The line above the 45 degree line represents a 50 percent under-prediction bound.

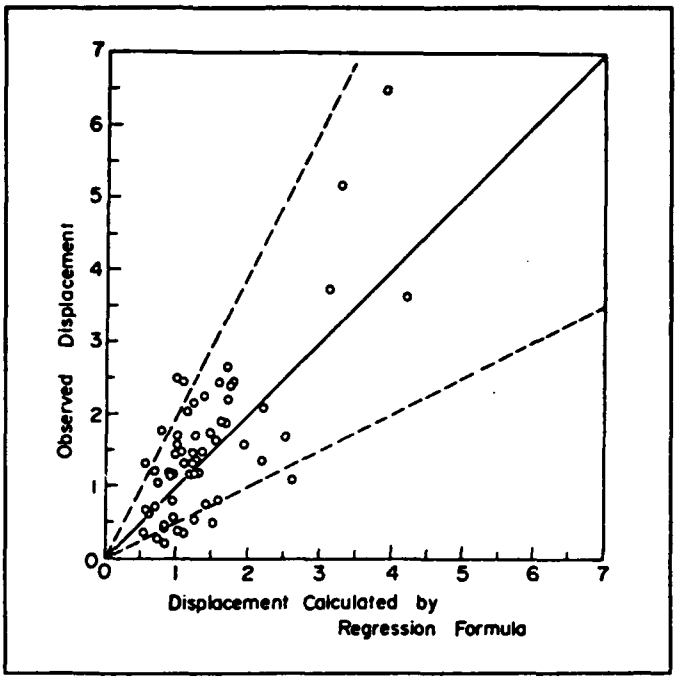

Figure 15 Measured Versus Predicted Displacement from Hamada et al., 1986, Regression Equation (after Hamada et al., 1986).

We digitized figure 15 and calculated the coefficient of correlation, r, for the measured versus predicted displacements. (Normally, the coefficient of determination, r^2, is used to compare the usefulness of a regression model. The coefficient of determination may be found squaring r). The value of r^2 for Hamada's model is approximately 0.58. In short, this means that the predictor variables (i.e., H and S) are explaining 58 percent of the variability found in the measured displacements.

To be consistent with Hamada's analysis, we used the Japanese Code of Bridge Design curves to calculate H. However, one of the basic assumptions of regression analysis is that the predictor variables can be measured without error (i.e., the value for the measurement can be exactly determined). H and S as used by Hamada et al., require some analysis or interpretation to quantify these factors. For example, H cannot be directly measured but is calculated from SPT and grain size data and applying the analysis outlined by

the Japanese Code of Bridge Design. H was then interpolated and extrapolated from borehole to borehole (see figure 6 and profiles in appendix) to establish a mean thickness for a displacement block.

Additionally, S, as defined by Hamada et al., requires that the larger value of the ground slope or slope of the bottom of the liquefied zone be used. In cases where a free face was present, Hamada et al., steepened their measurement of slope into the channel bottom. Obviously, there is some interpretation involved in S, especially when topographical relief is undulating or when a displacement has occurred at the base of a hill or near a depression or channel. Also, the slope of the bottom of the liquefied zone is subject to interpretation largely due to interpolation and extrapolation of this boundary between boreholes.

In order to corroborate Hamada's model and see if our reduction of H and S is consistent with their study, we independently determined H and S from the SPT logs and profiles and applied them to Hamada's model to predict measured displacements at Niigata and Noshiro. For S, we used the greater value of the ground slope or the slope to the base of the free face if one existed. This measurement of S is similar to that of Hamada et al., except that we neglected to use the slope of the base of the liquefied layer for cases where it exceeded the ground slope.

The r^2 for measured versus predicted displacements from our reduction of H and S was significantly lower than the r^2 reported by Hamada (0.1 compared with 0.58). Our lower result may indicate: 1) our reduction of the SPT and profile data to determine H and S may not be consistent with the methods used by Hamada et al. Because some interpretation is involved in obtaining the independent variables H and S, we are obviously introducing considerable

error by our methods of estimating H and S, and 2) the use of ground slope instead of the slope of the bottom of the liquefied zone may produce poorer estimates of displacement for cases where the latter slope is steeper than the former.

To evaluate the performance of Hamada's equation for predicting displacements at U.S. liquefaction sites, we used it to predict the measured displacements compiled by our research. Figure 16 is a scatter plot of the measured versus predicted displacements for U.S. and Japanese sites. There is a poor prediction for some of the U.S. sites. Some possible reasons for the poorer predictions are:

1) Seismic conditions for our U.S. case studies vary significantly from those seismic conditions reported for Niigata and Noshiro Cities and Juvenile Hall. Niigata and Noshiro Cities (which make up more than 90 percent of the data set), experienced relatively similar magnitudes earthquakes (7.5 and 7.7 respectively) and maximum site accelerations (0.16 and 0.25 g). Our set of U.S. case studies includes earthquake magnitudes which range from 6.6 to 9.2 M_w and site accelerations from 0.09 to 0.60 g. Furthermore, earthquake magnitude, maximum site acceleration and duration of ground shaking may influence ground displacement beyond the influence incorporated in defining H. (Note: Earthquake magnitude and maximum acceleration are used in Japanese Code of Bridge Design to calculate the thickness of the liquefied zone). H, as thus defined, combines the influence of soil and seismic factors on displacement. Perhaps, the use of another layer factor (which is independent of earthquake magnitude and maximum acceleration) and the

inclusion of a seismic factor in the model will improve predictions for a wider range of seismic conditions.

2) Particle size of the liquefied soil appears to affect displacement. The soils that liquefied in Japan were relatively thick homogeneous deposits of clean, uniformly-graded medium sand. In contrast, U.S. sites display a spectrum of liquefied soil types: from sand to silty sand to silt and from gravel to sandy gravel to silty gravel. For example, displacements were greatly over-predicted for gravelly U.S. sites such as Whiskey Springs and Pence Ranch. Also, displacements were over-predicted for some U.S. silty sites such as Heber Road and Wildlife. Mean grain size should be included in the model.

3) Our techniques for estimating H and S for U.S. sites may not be consistent with those of the Japanese investigators.

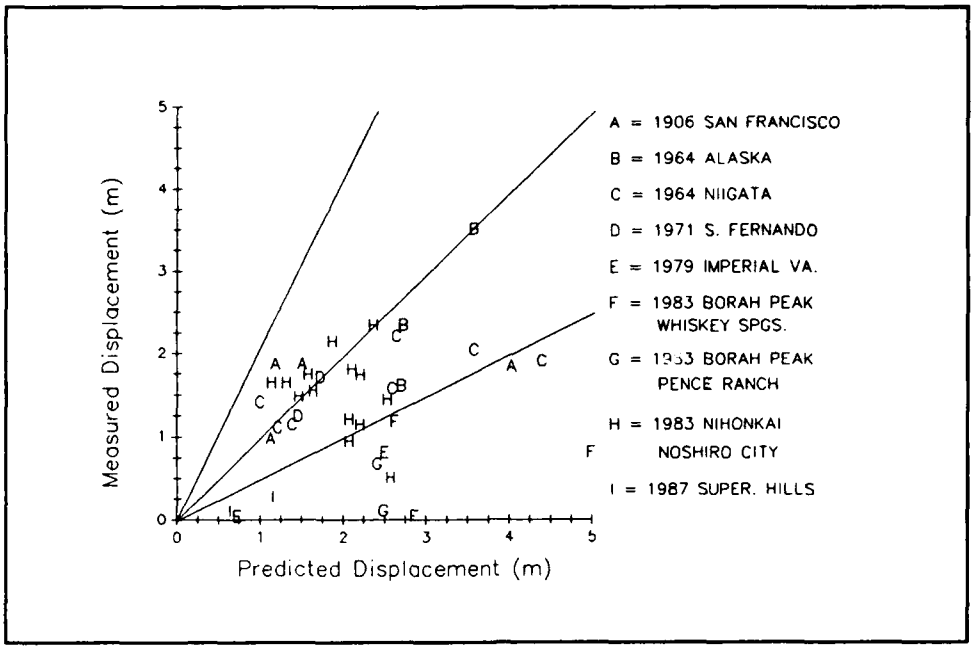

Figure 16 Measured Versus Predicted Displacement from Hamada et al.,1986 Regression Equation for U.S. and Japanese Liquefaction Sites.

In summary, the equation proposed by Hamada et al., appears to yield reasonable predictions for liquefaction sites experiencing 7.5 M earthquakes and comprised of relatively clean, medium grained sands. However, extrapolation of the Japanese regression equation beyond these conditions may yield poorer predictions. Additionally, there is interpretation involved in defining S which introduces error into the regression analysis and may result in poorer predictions.

CHAPTER 5: SUMMARY AND CONCLUSIONS

Considerable progress has been made since the 1964 Niigata and 1964 Alaskan earthquakes in understanding the liquefaction process and predicting its occurrence. However, only limited progress has been made in developing methods for estimating ground failure displacement resulting from liquefaction. The principal task of this study was to compile case history data from several major earthquakes in order to develop a database to study liquefaction induced ground failure. Several seismic, geological, stratigraphic, soil and engineering factors were defined and tabulated from case studies of lateral spreads. Measurements were tabulated for the 1906 San Francisco, 1964 Alaska, 1964 Niigata, 1971 San Fernando, 1979 Imperial Valley, 1983 Borah Peak, 1983 Nihonkai-Chubu and 1987 Superstition Hills earthquakes.

Youd and Perkins, 1987, with the liquefaction severity index, LSI, formulated one of the first empirical relationships to predict horizontal ground failure displacement. They postulated that amount horizontal ground failure displacement at a site is directly related to the intensity of the ground shaking and its duration and that both of these variables are ultimately functions of the earthquake magnitude and the distance to the zone of earthquake energy release. Youd and Perkins 1987 also listed several site properties that may influence the amount of horizontal ground failure displacement. Because site data was not available for most of the case histories they considered, they selected a single geologic environment in an attempt to minimize site condition variability. Their liquefaction severity index, LSI, is based on the maximum reported ground failure displacement on

lateral spreads within the type setting and is expressed as a function of earthquake magnitude and distance to the energy source.

Ishihara, 1985, showed that liquefaction induced ground failure is related to the thickness of the overlying sediment and the thickness of the liquefied layer. Hamada et al, 1986, using standard penetration data and slope measurements, formulated an empirical equation to predict horizontal ground failure displacement from the slope and thickness of the liquefied zone.

The estimation of horizontal ground failure displacement is a complex problem which involves the consideration of both seismic and site factors. The Youd - Perkins model emphasizes seismic factors (magnitude and distance to the source) and attempts to normalize the affects of site factors. In contrast, the empirical model proposed by Hamada et al., 1986, emphasizes some site factors such as slope and thickness of the liquefiable layer, but does not consider the influence of seismic factors. We have used the concepts of these workers and observations from the review of several liquefaction induced ground failures to formulate more comprehensive models based on seismic and site factors to predict horizontal ground failure displacement.

Preliminary regression analyses were made of the compiled data in the case histories to test preliminary models that predict horizontal ground displacement. Preliminary results indicate that models which include strong ground motion duration, thickness of the liquefied zone and the depth to the top of the liquefied zone are significant at the 99 percent confidence level. It also appears that the thickness of the liquefied zone is better predictor of horizontal ground displacement than any of the various $(N_1)_{60}$ factors tested. This suggests that larger horizontal displacements can be expected

where thicker layers of liquefiable sediments exist.

Models that include acceleration and duration for the seismic predictor variables gave slightly better results those that used magnitude and distance for the seismic predictor variables. However, this result is preliminary and could change with further analyses. Some of the maximum ground accelerations and most of the strong motion durations reported by this study for the various sites were calculated from magnitude - distance relationships. This fact might suggest that the acceleration - duration models might be ultimately expressed as magnitude - distance models.

The effects of ground slope and the presence of a free face on horizontal ground displacement could not be adequately modeled from the researched data set. The geometry of the free face and its relationship with the liquefied layer need to be more rigorously defined and measured. Grain size of the liquefiable sediments also apparently affects displacement and should be included in the empirical model.

More research is needed to refine and extend the case histories presented in the study. In addition, more refined measurements of key factors is needed to reduce error in the data set and to improve the statistical significance of the predictor variables used in the preliminary models. We are encouraged by the partial success that empirical models have shown and look forward to the time when more comprehensive models give the practicing engineer an adequate means to assess the potential severity of liquefaction induced ground failure.

REFERENCES

Andersen, K. H., 1983, "Report, Foundation Analyses for Gravity Platforms - Stability, Soil Stiffness and Settlements," Lecture presented at the NIF Course, "Fundamentberegninger for Gravitasjonsplattformer," Fagerness 5.-7.12.1983, December, 1983, Norwegian Geotechnical Institute, Oslo, Norway.

Andrus, R. D., 1988, Investigation and Liquefaction Analysis at Pence Ranch, Ch. 4, Ph.D. Dissertation, Unversity of Texas at Austin, preliminary.

Andrus, R. D., and Youd, L. T., 1987, "Subsurface Investigation of Liquefaction - Induced Lateral Spread Thousand Springs Valley, Idaho," U. S. Army Corp of Engineers, Miscellaneous Paper GL-87-8, p. 106.

Andrus, R. D., and Youd, T. L., 1989, "Penetration Tests in Liquefiable Gravels,"Proceedings of the 12th International Conference on Soil Mechanics and Foundation Engineering, A. A. Balkema, Publishers, Vol. 1, pp. 679 -682.

Bartlett, S. F., Youd, T. L., 1989a, "Compiliation of Case Histories of Ground Failure Displacement Associated with Soil Liquefaction," Brigham Young University Civil Engineering Department Report No. CEG 89-01.

Bartlett, S. F., Youd, T. L., 1989b, "Case Studies of Liquefaction Induced Ground Failures," Address to the Symposium on Earthquake-Induced Landslides, Joint Meetings of the Cordilleran and Rocky Mountain Sections, Geological Society of America, Spokane, Washingtion, May 8 - 11, 1989.

Bennett, M. J., 1988, "Liquefaction Analysis of the San Fernando Valley Juvenile Hall, California," U. S. Geological Survey Open File Report 81-502, p. 83.

Bennett, M. J., 1989, "Liquefaction Analysis of the 1971 Ground Failure at the San Fernando Valley Juvenile Hall, California," Bulletin of the Association of Engineering Geologists, Vol. XXVI, No. 2, pp. 209-226.

Bennett, M. J., Youd, T. L., Harp, E. L., and Wieczorck, G. F., 1981, "Subsurface Investigation of Liquefaction, Imperial Valley Earthquake, California, October 15, 1979," U.S. Geological Survey Open File Report 81-502, p. 83.

Bennett, M. J., McLaughlin, P. V., Sarimento, J. S., and Youd, T. L., 1984, "Geotechnical Investigation of Liquefaction Sites, Imperial Valley, California, U. S. Geological Survey Open File Report 84-252, p. 103.

Bouckovalas, G., Whitman, R. V., Marr, W. A., 1984 "Permanent Displacement of Sand with Cyclic Loading," Journal of Geotechnical Engineering, ASCE, Vol. 110(11), pp. 1606 - 1623.

Campbell, K. W., 1985, "Strong Motion Attenuation Relations: A Ten-Year Perspective," Earthquake Spectra, Vol. 1, No. 4, pp. 759 - 804.

Casagrande, A., 1936, "Characteristics of Cohesionless Soils Affecting the Stability of Slopes and Earth Fills," Journal of the Boston Society of Civil Engineers, Jan. 1936, Reprinted in Contributions to Soil Mechanics 1925 to 1940, Boston Society of Civil Engineers, Oct. 1940, pp.257 - 276.

Casagrande, A., 1938, "The Shearing Resistance of Soils and its Relation to the Stability of Earth Dams," Proceedings, Soils and Foundation Conference of the U. S. Engineer Department, 1938.

Castro, G., 1969, "Liquefaction of Sands" Harvard Soil Mechanics, Serial No. 81, p. 112.

Castro, G., 1975, "Liquefaction and Cyclic Mobility of Saturated Sands," Journal of the Geotechnical Engineering Division, ASCE, Vol. 101, No. GT6, pp. 551 - 569.

Castro, G., Poulos, S. J., 1977, "Factors Affecting Liquefaction and Cyclic Mobility," Journal of the Geotechnical Engineering Division, ASCE, 103(GT6), pp. 501 - 506.

Castro, G., Poulos, S. J., France, J. W. and Enos, J. L., 1982, "Liquefaction Induced by Cyclic Loading." Report to National Science Foundation, Geotechnical Engineers, Inc., Winchester, Massachusetts.

Chen, A. T. F., 1988, "On Seismically Induced Pore Pressure and Settlement," Earthquake Engineering and Soil Dynamics II, Recent Advances in Ground-Motion, ASCE Publication No. 20, pp. 482 - 492.

Crouse, C. B., and Turner, B. E., 1980, "Processing and Analysis Japanese Accelerograms and Comparisons with U.S. Strong Motion Data," Proceedings, 7th World Conference on Earthquake Engineering, Istanbul, Turkey, Vol. 2, p. 419-426.

Finn, W. D. L., 1980, "Seismic Deformations in an Underwater Slope," Report to Earth Technology Corporation.

Finn, W. D. L., 1982, "Computation of Seismically Induced Settlements in Sands," Preliminary Report to U.S. Army Corps of Engineers, Waterways Experiment Station, Vicksburg Mississippi.

Finn, W. D. L., 1984, "Progress Reports," U.S. Army Corps of Engineers Office of Standardization, London.

Finn, W. D. L., 1985a, "Dynamic Analysis of EPR Gravity Platform,"Report to Exxon Production Research Company.

Finn, W. D. L., 1985b, "Permanent Deformations in Lornex Tailings Dam, Preliminary Feasibility Study," Report to Klohn Leonoff Consultants Ltd.

Finn, W. D. L., 1988, "Dynamic Analysis in Geotechnical Engineering," Earthquake Engineering and Soil Dynamics II, Recent Advances in Ground-Motion Evaluation, ASCE Publication No. 20, pp. 523 - 591.

Goa Z. Hu, B., Chang, D., 1983, "Some Geological Considerations for the Damage During the Tangshan Earthquake," North China Earthquake Sciences, Vol. 1, pp. 64 - 72 (In Chineses).

Goodman, R. E., Seed, H. B., 1966, "Earthquake-Induced Displacements in Sand Embankments, Journal of the Soil Mechanics and Foundations Division, ASCE 92(SM2), pp. 125 - 146.

Hamada, M., Yasuda, S., Isoyama, R., and Emoto, K., 1986, "Study on Liquefaction Induced Permanent Ground Displacements," Published by the Association for the Development of Earthquake Prediction in Japan, p. 87.

Hamada, M., Towhata, I., Yasuda, S., Isoyama, R., 1987, "Study of Permanent Ground Displacement Induced by Seismic Liquefaction," Computers and Geotechnics, Vol. 4, No. 4, Elsevier Applied Science Publishers, pp. 197 - 220.

Hamada, M., Yasuda, S., Wakamatsu, K., 1988, "Case Study on Liquefaction-Induced Ground Failures during Earthquakes in Japan," Proceedings, First Japan -U.S. Workshop on Liquefaction, Large Ground Deformation and Their Effects on Lifeline Facilities, pp. 3 - 21.

Hardman, S. L., and Youd, T. L., 1987, Mapping the Extent and Thickness of Liquefiable Soil Layers at Engineering Sites, U. S. Army Corp of Engineers, Miscellaneous Paper S-73-1, p. 161.

Holzer, T. L., Youd, T. L., Bennett, M. J., 1988, "In Situ Measurement of Pore-Pressure Build-Up During Liquefaction," 20th Joint UJNR Panel on Wind and Seismic Effects, p. 17.

Holzer, T. L., Youd, T. L, Hanks, T. C., 1989, "Dynamics of Liquefaction During the 1987 Superstition Hills, California, Earthquake," Science, Vol. 244, pp. 56 - 59.

Idriss, I. M., Seed, H. B., 1968, "Seismic Response of Horizontal Soil Layers," Journal of the Soil Mechanics and Foundations Division, ASCE, Vol. 94, No. SM4, pp. 1003 - 1031.

Ishihara, K., 1985, "Stability of Natural Deposits During Earthquakes," Proceedings of the Eleventh International Conference on Soil Mechanics and Foundation Engineering, Vol. 1, pp. 321 - 376.

Iwasaki, T., Tatusoka F., Tokida, K., and Yasuda S., 1978, "A Practical Method for Assessing Soil Liquefaction Potential Base on Case Studies at Various Sites in Japan," Proceedings of the Fifth Japan Earthquake Engineering Symposium, (in Japanese).

Joyner, W. B., and Boore, D.M., 1981, "Peak Horizontal Acceleration and Velocity from Strong Motion Records Including Records from the 1979 Imperial Valley, California Earthquake," Bulletin of the Seismological Society of America, Vol 71, No. 6, pp.2011 - 2038.

Joyner, W. B., and Boore, D. M., 1988, "Measurement, Characterization and Prediction of Strong Ground Motion," Earthquake Engineering and Soil Dynamics II, Recent Advances in Ground Motion Evaluation, ASCE, No. 20, pp. 43 - 102.

Kachadoorian, R., 1968, "Effects of the Earthquake of March 27, 1964 on the Alaska Highway System," U. S. Geological Survey Professional Paper 545-C, p. 66.

Kanamori, H., 1978, "Quantification of Earthquakes," Nature, Vol. 271, p. 411 - 414.

Kokusho, T., Yoshida, Y., Esashi, Y., 1983, "Evaluation of Seismic Stability of Dense Sand Layer (Part 2), - Evaluation Method by Standard Penetration Test," Report 383026, Central Research Institute for Electric Power Industry, Tokyo Japan.

Krinitzsky, E. L., Chang, F. K., 1988a, "Intensity-Related Earthquake Ground Motions," Bulletin of the Association of Engineering Geologists, Vol. XXV, No. 4, pp. 425-435.

Krinitzsky, E. L., Chang, F. K., 1988b, "Magnitude-Related Earthquake Ground Motions," Bulletin of the Association of Engineering Geologists, Vol. XXV, No. 4, pp. 399-423.

Ledbetter, R., 1983, "Current Methodologies for Assessing Seismically Induced Settlements in Soil," U. S. Nuclear Regulatory Commission Publication NRC Fin B7002, p. 54.

Li-San, H., Hammack, J., 1984, "The Japan Sea Control Region Tsunami of May 26, 1983," National Academy Press, Washington D. C., p. 33.

Liao, S. S. C., 1986, "Statistical Modeling of Earthquake-Induced Liquefaction," Ph.D. Dissertation, Department of Civil Engineering, Massachusetts Institute of Technology, p. 470.

Makdisi, F. I., Seed, H. B., 1978, "Simplified Producedure for Estimating Dam and Embankment Earthquake-Induced Deformations," Journal of the Geotechnical Engineering Division, ASCE 104(GT7), pp. 849 - 867.

Marr, W. A., Christian, J. T., 1981, "Permanent Displacements Due to Cyclic Wave Loading," Journal of the Geotechnical Engineering Division, ASCE, Vol. 107(GT8), pp. 1129 - 1149.

Marr, W. A., Urzua, A., Bouckovalas, G., 1982, "A Numerical Model to Predict Permanent Displacement from Cyclic Loading of Foundations," Proceedings of the Third International Conference on the Behavior of Offshore Structures, Vol. 1, McGraw Hill/Hemisphere Publishing Company, New York, New York, pp. 297 - 312.

Martin, G. R., Finn, W. D. L., Seed, H. B., 1975, "Fundamentals of Liquefaction Under Cyclic Loading," Soil Mechanics Series Report No. 23, Department of Civil Engineering, University of British Columbia, Vancouver; also Proc. Paper 11284, Journal of Geotechnical Engineering Division, ASCE, Vol. 101, No. GT5, pp. 324 - 438.

McCulloch, D. S., Bonilla, M. G., 1970, "Effects of the Earthquake of March 27, 1964 on the Alaska railroad," U. S. Geological Survey Professional Paper 545-D, p. 161.

National Research Council, 1985, Liquefaction of Soils During Earthquakes, National Academy Press, Washington D. C., p. 240.

Newmark, N. M., 1965, "Effects of Earthquakes on Dams and Embankments," Geotechnique, 15(2), pp. 139 - 160.

Page, R. A., Boore, D. M., Joyner, W. B., Coulter, H. W., 1972, "Ground Motion Values for Use in Seismic Design of the Trans-Alaska Pipeline System," U. S. Geological Survey Circular 672, p. 16.

Poulos, S. J., 1971, "The Stress-Strain Curves of Soils," unpublished paper, available from Geotechnical Engineers, Inc., Winchester, Massachusetts.

Robertson, P. K., Campanella, R. G., and Wightman, A., 1983, "SPT-CPT Correlations," Journal of Geotechnical Engineering, Vol. 109, pp. 1449 - 1459.

Ross, G. A., Seed, H. B. and Migliaccio, R. R., 1969, "Bridge Foundation Behavior in Alaska Earthquake," Journal of the Soil Mechanics and Foundations Division, ASCE, Vol. 95, No. SM4. pp. 1007 - 1036.

Seed, H. B., Idriss, I. M., 1970, "Soil Moduli and Damping Factors for Dynamic Response Analyses," Report No. EERC 70-10, Earthquake Engineering Research Center, University of California, Berkeley.

Seed, H. B., 1979, "Soil Liquefaction and Cyclic Mobility Evaluation for Level Ground during Earthquakes," Journal of the Geotechnical Engineering Division, ASCE, Vol. 105, No. GT2, pp. 201 - 255.

Seed, H. B., 1987, Design Problems in Soil Liquefaction, Journal of Geotechnical Engineering, Vol. 113, No. 8, pp. 827-845.

Seed, H. B., and Idriss, I. M., 1971 "Simplified Procedure for Evaluation of Soil Liquefaction Potential," Journal of Soil Mechanics and Foundations Division, ASCE, Vol. 97, No. SM9, pp. 1249 - 1273.

Seed, H. B., Lee, K. L., Idriss, I. M., Makdisi, F., 1973, "Analysis of the Slides in the San Fernando Dams During the Earthquake of Feb. 9, 1971," Report No. EERC 73-2, Earthquake Engineering Research Center, University of California, Berkeley.

Seed, H. B., Idriss, K. L., Lee, K. L., Makdisi, F. I., 1975, "Dynamic Analysis of the Slide in the Lower San Fernando Dam During the Earthquake of February 9, 1971," Journal of the Geotechnical Engineering Division, ASCE, Vol. 101(GT9), pp. 889 - 911.

Seed, H. B. and Idriss, I. M., 1982, Ground Motions and Soil Liquefaction During Earthquakes, Earthquake Engineering Research Institute Monograph, p. 134.

Seed, H. B., Idriss, I. M., Arrango, I., 1983, "Evaluation of Liquefaction Potential Using Field Performance Data," Journal of Geotechnical Engineering, ASCE, Vol. 109(3), pp. 458 - 482.

Seed, H. B., Tokimatsu, K., Harder, L. F., and Chung, R. M., 1984, "The Influence of SPT Procedures in Soil Liquefaction Resistance Evaluations," Report No. UBC/EERC-84/15, Earthquake Engineering Research Center, University of California, Berkeley California.

Seed, H. B., Tokimatsu, L. F., Harder, L. F., and Riley, M. C., 1985, "Influence on SPT Procedures in Soil Liquefaction Resistance Evaluations." Journal of Geotechnical Engineering, ASCE, Vol. III, No. 12, pp. 1425 - 1446.

Seed, H. B., and De Alba, P., 1986a, "Use of SPT and CPT Tests for Evaluating the Liquefaction Resistance of Sands," Use of In-Situ Tests in Geotechnical Engineering, ASCE, Geotechnical Special Publication No. 6, pp. 281 - 302.

Seed, H. B., Wong, R. T., Idriss, I. M., Tokimatsu, K., 1986b, "Moduli and Damping Factors for Dynamic Analyses of Cohesionless Soils," Journal of the Geotechnical Engineering Division, ASCE, Vol. 112, No. 11, pp. 1016-1032.

Shibata, T., 1981, "Relations Between N-value and Liquefaction Potential of Sand Deposits," Proceedings of the Sixteenth Annual Convention of Japanese Society of Soil Mechanics and Foundation Engineering, pp. 621 - 624.

Taniguchi, E., 1983, "Prediction of Earthquake Induced Deformation of Earth Dams," Soils and Foundations, Vol. 23(4), pp. 126 -132.

Terzaghi, K., and Peck, R. B., 1948, Soil Mechanics in Engineering Practice, New York, John Wiley and Sons, p. 566.

Tokimatsu, K., Yoshimi, Y., 1983, "Empirical Correlation of Soil Liquefaction Based on SPT N-Value and Fines Content," Soils and Foundations, Japanese Socity of Soil Mechanics and Foundation Engineering, Vol. 23(4), pp. 56 - 74.

Tokimatsu, D., Seed, H. B., 1987, "Evaluation of Settlements in Sands due to Earthquake Shaking," Journal of Geotechnical Engineering, ASCE, Vol. 113, No. 8, pp. 861 - 878.

VanMarcke, E. H., Lai, S. P., 1980, Strong Motion Duration and RMS Amplitude of Earthquake Records," Bulletin of the Seismological Society of America, Vol. 70, No. 4, pp. 1293 -1307.

Youd, T. L., 1972, "Compaction of Sands by Repeated Shear Straining," Journal of the Soil Mechanics and Foundations Division, ASCE, SM 7, pp. 709 - 725.

Youd, T. L., 1973, "Liquefaction, Flow, and Associated Ground Failure," U. S. Geological Survey Circular 688, p. 12.

Youd, T. L., 1977, "Packing Changes and Liquefaction Susceptibility," Journal of the Geotechnical Engineering Division, ASCE, Vol. 103, No. GT8, pp. 918 - 922.

Youd, T. L., 1978, "Major Cause of Earthquake Damage is Ground Failure," Civil Engineering-ASCE, April 1978, pp. 47 - 51.

Youd, T. L., 1985, Brigham Young University Civil Engineering Department Memorandum, Dec. 26, 1985.

Youd, T. L., 1989, "Ground Failure Damage to Buildings during Earthquakes," Foundation Engineering: Current Principles and Practices, Vol. 1, Proceeding of the Congress sponsored by the Geotechnical Engineering Division of ASCE, Evanston Illinois, June 25 - 29, 1989, pp. 758 - 770.

Youd, T. L., and Hoose, S. N., 1976, "Liquefaction During 1906 San Francisco Earthquake," Journal of the Geotechnical Engineering Division, Vol. 102, No.GT5, pp. 425 - 439.

Youd, T. L., and Hoose, S. N., 1978, "Historic Ground Failures in Northern California Triggered by Earthquakes," U. S. Geological Survey Professional Paper 993. p. 177.

Youd, T. L., and Perkins, D. M., 1978, "Mapping Liquefaction-Induced Ground Failure Potential," Journal of the Geotechnical Engineering Division, ASCE, Vol. 104, No. GT4, April, 1978, pp. 433 - 446.

Youd, T. L., and Bennett, M. J., 1981, "Liquefaction Studies Following 1979 Imperial Valley Earthquake," ASCE Preprint 81-544, Session No. 24, 1981 ASCE ational Convention.

Youd, T. L., and Bennett, M. J., 1983, "Liquefaction Sites, Imperial Valley, California," Journal of Geotechnical Engineering, Vol. 109, No. 3, pp. 440 - 457.

Youd, T. L., Harp, E. L., Keefer, D. K., and Wilson, R. C., 1985, "The Borah Peak, Idaho Earthquake of October 28, 1983," Earthquake Spectra, Vol. 2, No. 1, pp. 71 - 89.

Youd, T. L., and Perkins, D. M., 1987, "Mapping of Liquefaction Severity Index," Journal of Geotechnical Engineering, Vol. 113, No. 11, pp. 1374 - 1392.

Youd, T. L., Bartlett, S. F., 1988, "U.S. Case Histories of Liquefaction-Induced Ground Displacement," Proceeding, First Japan - U.S. Workshop on Liquefaction, Large Ground Deformation and Their Effects on Lifeline Facilities, pp. 22 -31.